ROLES OF ALPHA-ACTININ IN THE REGULATION OF MITOTIC SPINDLE ORGANIZATION IN MAMMALIAN CELLS

Vinayaka Srinivas

(M.Sc., Bangalore University)

A THESIS SUBMITTED
FOR THE DEGREE OF DOCTOR OF PHILOSOPHY
TEMASEK LIFE SCIENCES LABORATORY
NATIONAL UNIVERSITY OF SINGAPORE
2013

Acknowledgements

This thesis would not have materialized if not for the contribution of many people. Firstly, I'd like to acknowledge and thank Dr. Maki Murata-Hori, for her invaluable patience, guidance, and unbending encouragement. Dr. Maki has been instrumental in my training and this project would have been an impossible task without her support. Research is inherently a cycle of ups and downs, and it was her tenacity that taught me to keep going through all these times.

I am also immensely grateful to Prof. Mohan Balasubramanian for serving as my thesis committee member during the early stages of my project and for taking me in during the final year of my PhD. I would also like to acknowledge the other members of my thesis advisory committee, Dr. Cynthia He and Dr. Liou Yin Cherng, for their insights and suggestions that helped shape the course of my work.

For the generous funding, facilities, and technical support, I would like to thank to Temasek Life Sciences Laboratory (TLL). More importantly, I am thankful to the people in TLL – Dr. Svetlana Mukhina, Dr. Ramirez Hernandez Tzutzuy, Dr. Xiaodong Zhu, Dr. Kian Hong, Dr. Veena, Shyan, Shaz, Lu Ting, Ranjay, Ivan, Adrian, Keiko, Pooisan, Dhivya, Pooja, Qimei, Yishi and other past members in the Maki's lab.

I am especially thankful to a handful of friends including Bianx, Hong Xin, Ram, and Dr. Junxia Wang for making my stay in Singapore a very memorable one.

To all my friends in Singapore and India, I'd like to express my thanks for the constant emotional support during my stay in Singapore.

Last but not least, I would like to express my heartfelt gratitude to my late parents – Srinivas and Padma, my brother babu and my sisters Hema, Divya, Gayathri, and all other family members for always believing in me and for loving me selflessly.

Table of contents

Summary

Cytokinesis is the last step in cell cycle, where a single mother cell divides to give to rise to two daughter cells. Proper spatiotemporal regulation of cytokinesis is crucial for the faithful segregation of the genetic material into the daughter cells. Proper understanding of this process enables us to detect and identify reasons behind many of the diseases as well as in designing effective control measures for these diseases. Recent studies in various model organisms including yeast, *C. elegans*, and mammalian cells unravelled many mysteries pertaining to the mechanism of cytokinesis. This led to the current understanding of the process of cytokinesis, which is divided into four different stages: 1) positioning of the cleavage furrow between the separated chromosomes, 2) assembly of the actomyosin-based contractile ring, which is one of major components of the cleavage furrow, 3) constriction of the contractile ring by the force generated by myosin II motors, and 4) division of the cell into two daughter cells.

Extensive research in the last few decades had led to the improved understanding of the process of cytokinesis at the molecular level and of the different pathways involved during cytokinesis. However, many open questions remain unanswered. Active research in the last few years had focused mainly on the biophysical aspects of the cell and its role in cytokinesis, and this led to a paradigm shift in cytokinesis with respect to the flow of events. The previously held idea that cytokinesis occurs in a straightforward biochemical pathway leading to cell division has been

rethought and current understanding considers mechanical feedback loop mechanism along with biochemical pathway to be cruicial for proper cell division. This change in perspective was ushered in by active studies on cell mechanics, stress generation and sensing by myosin II-based contractility, and control of regulatory proteins.

One of the main focuses in understanding the mechanical feedback loops regulating cytokinesis is the meshwork of the actin cortex. Actin had been extensively studied for its role during cytokinesis in the formation of the actomyosin and in other cellular process. The understanding of its function as a cell cortex component during cytokinesis gained attention only recently. Actin cytoskeleton is believed to be involved in a diverse range of processes mainly because of its ability to bind, interact and respond to a large pool of actin-binding proteins.

In my thesis project, using a combination of techniques including molecular manipulation and microscope-based techniques, I have uncovered a novel forl of actin crosslinking protein α-actinin during cytokinesis in mammalian cells was explored.

Successful cytokinesis requires proper positioning of cleavage furrow. Previous studies suggested that stable microtubules induce cortical ingression, whereas dynamic microtubules inhibit cortical ingression. However, the spatiotemporal regulation of microtubule dynamics is not clearly understood. This study experimentally established that α-actinin is important for the

regulation of mitotic spindle organization. This was demonstrated by the observation that α-actinin regulates microtubule dynamics by affecting the microtubule-actin cortex interaction in a myosin II-dependent manner. Alteration of the localization of microtubule-based cytokinetic regulators was further demonstrated to be affected by α-actinin. In conclusion, my study demonstrates that α-actinin is required to maintain the dynamic status of astral microtubules by preventing the recruitment of centralspindlin, but not CPC or PRC1, to astral microtubules.

List of Tables:

List of Figures:

List of Abbreviations:

Arp2/3	Actin-related protein 2/3
ATCC	American type culture collection
BSA	Bovine serum albumin
CB	Cytoskeletal buffer
CCD	Charge-coupled device
Cdc42	Cell division cycle 42
cDNA	Complementary DNA
DMEM	Dulbecco’s modified eagle medium
DMSO	Dimethyl sulfoxide
EB	End binding
ECT2	Epithelial cell transforming sequence 2 oncogene
EDTA	Ethylenediamine tetra acetic acid
FBS	Fetal bovine serum
F-actin	Filamentous actin
F12K	Ham's F12 K modification
GAP	GTPase activating protein
GAPDH	Glyceraldehyde-3-phosphate dehydrogenas
GBD	GTPase protein binding domain
GDI	guanine nucleotide dissociation inhibitor
GEF	Guanine nucleotide exchange factor
GDP	Guanosine-5-diphosphate
GFP	Green fluorescence protein
GTP	Guanosine-5-triohosphate

G-actin	Globular monomeric actin
HCl	Hydrocloric acid
HRP	Horseradish peroxidase
LB	Luria Bertani medium
MgcRacGAP	Homo sapiens Rac GTPase activating protein 1
MKLP	Mitotic kinesin like protein
MLC	Myosin light chain
mRFP	Monomeric red fluorescence protein
MRLC	Myosin regulatory light chain
NRK	Normal rat kidney
NA	Numerical aperture
PBS	Phosphate buffered saline
PFA	Paraformaldehyde
PRC	Protein regulator of cytokinesis
RhoA	Ras homolog gene family, member A
ROCK	Rho-associated kinase
siRNA	small interference RNA
shRNA	shrot hairpin or small hairpin RNA
SNARE	Soluble N-ethylmaleimide-sensitive factor attachment protein receptor
STE	Sodium Tris-EDTA
TCA	Trichloroacetic acid
TEMED	Tetramethylenediamine
Tris	2-amino-2(hydroxymethyl)-1,3-propandiol
Triton-X	Octylphenoxypolyethoxyethanol

α-actinin	alpha-actinin
α-tubulin	alpha-tubulin
β-tubulin	beta-tubulin

1 Introduction

1.1 Cell cycle and Cell division:

1.1.1 *Cell cycle progression*

Growth and reproduction are an absolute necessity for all living organisms. Cells, the basic entity of all living forms, undergo a process known as cell cycle in order to grow and reproduce. The cell cycle follows a series of phases consisting of: G1 (Gap), S (Synthesis), G2 (Gap) and M (Mitosis) (Figure 1). The first three phases are collectively known as Interphase and contributes to ~90% of the duration of cell cycle in most cells. Progression of the cell cycle is under the control of the oscillating expression levels of Cdks and their substrates cyclins (Figure 1, Wheatley *et al.*, 1997; Shuster and Burgess, 1999).

The M phase consisting of mitosis and cytokinesis is the last stage of the cell cycle where a single mother cell is faithfully divided into two daughter cells. Mitosis can be divided into five different stages: prophase, prometaphase, metaphase, anaphase and telophase. Prophase is characterized by chromatin condensation and centrosomal migration to opposite poles. Prometaphase is marked by nuclear envelope breakdown. Microtubules emanated from centrosomes start attaching to chromosomes and pushing them towards the centre of the cell. At metaphase, chromosomes are aligned at the metaphase plate. During anaphase, the duplicated chromosomes are separated towards

the opposite centrosomes. In telophase, the chromosomes are decondensed and the nuclear envelope begins to reform around the decondensed chromosomes while cytokinesis occurs and two daughter cells are produced. The entire events of the cell cycle repeat in both daughter cells (Alberts et al. The Molecular Miology of the Cell, the 4th Edition).

Figure 1: Schematic of overview of cell cycle stages in eukaryotic cells.

G1, S and G2 are collectively referred to as Interphase, which is followed by M phase. M phase consists of mitosis and cytokinesis. Progression through different cell cycle stages is regulated by different Cdks and cyclins.

1.1.2 Cytokinesis

Cytokinesis is the final step of cell division, where a single mother cell is physically separated into two daughter cells. In fission yeast and animal cells, cytokinesis can be subdivided into four sequential steps: 1) determination of the position of the cleavage furrow, 2) assembly of the contractile ring, 3) constriction of the contractile ring, and 4) abscission. As seen in the following chapters which describes cytokinesis in fission yeast (*S.Pombe)* and animal cells respectively, we will be able to appreciate how a common event can be executed by different mechanisms.

1.1.2.1 Cytokinesis in Fission yeast

1.1.2.1.1 *Determination of the position of the division site*

In fission yeast *S. pombe*, the division site selection process is dependent on several important factors including cellular morphology, the position of the nucleus and proteins involved in the ring assembly (Paoletti and Chang, 2000; Sipiczki *et al.*, 2000; Tolic-Nørrelykke *et al.*, 2005). The division site is determined during late G2 phase. The nucleus-localized protein Mid1p relocates to a region underlying the plasma membrane into a cortical band (Sohrmann *et al.*, 1996; Bähler *et al.*, 1998). It has been shown that Mid1p localization is regulated by Polo-like kinase 1, which is a conserved family of ser/thr mitotic kinase and is involved in centrosome maturation and the mitotic

spindle formation. It also plays a role during late stage of mitosis and cell division (Glover *et al.*, 1996). Polo-like kinase 1 directly interacts with type II myosin myo2p and promotes the equatorial localization of other cytokinetic ring components including Myo2p, Rng2p, Cdc4p and F-actin (Bähler *et al.*, 1998; Wu *et al.*, 2003; Motegi *et al.*, 2004).

1.1.2.1.2 *Contractile ring formation*

Upon entry into mitosis, Mid1p localizes to around 60-80 nodes in the equatorial cortex and recruits other components of the contractile ring to the cortical nodes (Wu *et al.*, 2006). These components include profilin Cdc3p, tropomyosin Cdc8p, formin Cdc12p, myosin assembly factor Rng3p and type two myosin heavy chain Myo2p. The formin protein Cdc12p further interacts and recruits the Arp2/3 complex, type 1 myosin, Myo1p and WASP-related protein Wsp1p to the division site. Recruitment of these proteins induce polymerization of actin either from 60-80 nodes on the cortex or from a large cluster of formins at 1-2 nodes on the medial site (Mishra and Oliferenko, 2008) and ultimately leads to the formation of the actomyosin ring at the division site.

Rng2p, a calponin homology domain protein localized to the nodes in a Mid1p depended manner, serves as a critical link between the Mid1p and other cortical node components with the actomyosin ring (Laporte *et al.*, 2011;

Padmanabhan *et al.*, 2011). F-actin, through its interaction with myosin II, condenses by interacting with neighbouring nodes to give rise to a ring-like structure by a process known as search-capture mechanism (Wu *et al.*, 2006; Mishra and Oliferenko, 2008; Vavylonis *et al.*, 2008).

1.1.2.1.3 *Ring constriction and abscission*

In *S. pombe*, ring contraction is immediately followed by membrane addition for septum formation. Proteins involved in exocytosis including SNARE components and Rab proteins are directed towards the division site. Enzymes involved in cell wall synthesis have also been observed in the division septa and were shown to be essential for formation of primary and secondary septa (Cheng *et al.*, 2002; Liu *et al.*, 2002). Drug treatment and mutant analysis of vesicular transport protein suggested that the septum deposition is directly involved in the constriction of the actomyosin ring (Le Goff *et al.*, 1999; Liu *et al.*, 1999; Liu *et al.*, 2000). After the contraction of the actomyosin ring and deposition of the septa, the cell finally is physically separated into two daughter cells.

1.1.2.2 Cytokinesis in animal cell

1.1.2.2.1 *Determination of the position of the cleavage furrow*

In contrast to fission yeast, the position of the cleavage furrow is determined after anaphase onset in animal cells.

In animal cells, microtubules are responsible for the determination of the position of the cleavage furrow. Pioneering experiments conducted on sand dollar eggs suggested that astral microtubules are responsible for determination of the position of cleavage furrow (Rappaport, 1961). In contrast, micromanipulation experiments performed in mammalian cells showed that midzone microtubules are responsible for the furrow positioning (Cao and Wang, 1996). Experiments in *C. elegans* embryos suggested that both astral and midzone microtubules were capable of determining the position of the cleavage furrow (Bringmann and Hyman, 2005). Similarly, an elegant micromanipulation study revealed that both sets of microtubules were able to induce the formation of the cleavage furrow in grasshopper spermatocytes (Alsop and Zhang, 2003). Canman *et al* proposed that dynamic microtubules at polar regions inhibit cortical ingression while stabilized microtubules at the equatorial region induce furrow ingression (Canman *et al.*, 2003).

How do microtubules stabilize specifically at the equatorial region during cytokinesis? There are three groups of the protein/the protein complexes, named the chromosome passenger complex (CPC), PRC1, and centralspindlin complex that are known to be involved in the regulation of dynamics of microtubules in the equatorial region during cytokinesis (Glotzer, 2009).

The chromosome passenger complex, CPC, is a multimeric protein complex consisting of aurora B kinase, INCENP, survivin and borealin. CPC is present in the nucleus in interphase. During prometaphase and metaphase, CPC is associated with chromosomes. After cells enter anaphase, it relocates from chromosomes to the equatorial microtubules and remained associated with these microtubules during cytokinesis. Perturbing the function of any of the CPC components affects the activity and localization of the other members of the complex, suggesting that the whole complex is necessary for its proper functioning during cytokinesis (Jeyaprakash *et al.*, 2007; Ruchaud *et al.*, 2007).

Protein related to cytokinesis (PRC1) is a member of MAP65 family of proteins, and was first discovered as a substrate of Cdk1 (Jiang *et al.*, 1998; Loïodice *et al.*, 2005; Janson *et al.*, 2007; Gaillard *et al.*, 2008). The members of MAP65 family of proteins are known for selective cross-linking of anti-parallel arrays of microtubules including PRC1 (Loïodice *et al.*, 2005; Janson *et al.*, 2007; Gaillard *et al.*, 2008; Bieling *et al.*, 2010). Upon the anaphase onset, PRC1 localizes to the midzone microtubules and stabilizes and bundles these microtubules (Zhu and Jiang, 2005). In cells depleted of PRC1, furrow ingressed but failed to undergo abscission, leading to the formation of the binucleated cell (Mollinari *et al.*, 2005), suggesting that PRC1 is crucial for proper progression of cytokinesis.

Centralspindlin is a hetero-tetrameric complex consisting of MKLP1 and MgcRacGAP in a 2:2 stoichiometric ratio (Mishima *et al.*, 2002; Pavicic-Kaltenbrunner *et al.*, 2007). MKLP1 was first identified as a protein associated with the mitotic spindle in mammalian cells, while MgcRacGAP was discovered as a new member of the Rho family GTPase activating protein (GAP) (Sellitto and Kuriyama, 1988; Nislow *et al.*, 1990; Touré *et al.*, 1998). These two proteins were identified in several other organism and they are named differently among different organisms: MKLP1 (vertebrates), ZEN4 (*C. elegans*), Pavarotti (*Drosophila*), and an upstream regulator of RhoA, a RhoGAP protein MgcRacGAP (vertebrates), CYK-4 (*C. elegans*), RacGAP50C (*Drosophila*). In the rest of this thesis, I refer to MKLP1 and MgcRacGAP for the components of centralspindlin unless otherwise stated. Mutation analysis of MKLP1 or MgcRacGAP caused a failure of assembly of midzone microtubules and cytokinesis failure, suggesting that centralspidlin is required for midzone microtubule assembly and cytokinesis (Powers *et al.*, 1998; Raich *et al.*, 1998; Severson *et al.*, 2000).

A GEF domain-containing protein Ect2 is known to form a complex with centralspindlin during cytokinesis in animal cells (Yüce *et al.*, 2005; Zhao and Fang, 2005; Kamijo *et al.*, 2006). The interaction of Ect2 with the N terminus of HsCYK 4 has been shown to be important for its localization to the midzone (Yüce *et al.*, 2005; Zhao and Fang, 2005; Chalamalasetty *et al.*, 2006; Kamijo *et al.*, 2006; Nishimura and Yonemura, 2006). Similar to centralspindlin, cells depleted of Ect2 causes failure of cytokinesis and formation of multinucleate cells (Saito *et al.*, 2004). Depletion of either one of

the components of centralspindlin causes a failure of Ect2 localization to the midzone (Yüce *et al.*, 2005; Zhao and Fang, 2005; Chalamalasetty *et al.*, 2006; Kamijo *et al.*, 2006; Nishimura and Yonemura, 2006). In contrast, centralspindlin localization is not affected by Ect2 depletion (Yüce *et al.*, 2005; Kamijo *et al.*, 2006; Nishimura and Yonemura, 2006), suggesting Ect2 is a downstream factor of centralspindlin.

These three groups of the protein/the protein complex influence each other. For example, aurora B (a component of CPC) phosphorylates MKLP1, promoting its oligomerization, which is important for its localization and bundling of microtubules (Douglas *et al.*, 2010).

1.1.2.2.2 *Assembly of the contractile ring*

The major component of the contractile ring is F-actin and myosin II.

There are two distinct mechanisms to assemble F-actin at the equatorial region. The first mechanism involves the transport of pre-existing F- actin to the equatorial region, the process of which is dependent on myosin II activity (Zhou and Wang, 2008) although myosin II localization to the equatorial cortex is independent of its ATPase activity (Zhou and Wang, 2008). The second pathway is the *de novo* assembly of F-actin that involves RhoA-dependent pathway (Li *et al.*, 2010).

The RhoA pathway promotes the formation of actomyosin ring through two main effector pathways. RhoA activates the formins during cytokinesis, which nucleates unbranched filaments of actin. This function of RhoA is conserved from *Aspergillus*, fission yeast to human cells (Castrillon and Wasserman, 1994; Imamura *et al.*, 1997; Tominaga *et al.*, 2000; Pelham and Chang, 2002; Severson *et al.*, 2002; Tolliday *et al.*, 2002; Peng *et al.*, 2003; Ingouff *et al.*, 2005; Watanabe *et al.*, 2008). RhoA also promotes activation of myosin II through two kinases, ROCK and Citron kinase (Amano *et al.*, 1996; Yamashiro *et al.*, 2003). Both kinases promote the activation of myosin II by directly phosphorylating the myosin regulatory light chain (Matsumura, 2005) and are involved in cytokinesis (Madaule *et al.*, 1998; Kosako *et al.*, 2000).

Apart from actin and myosin II, the contractile ring consists of other proteins including anillin, actin crosslinking proteins, septin filaments, specific lipids (Dobbelaere and Barral, 2004; Matsumura, 2005; Joo *et al.*, 2007; Maddox *et al.*, 2007; Reichl *et al.*, 2008; Estey *et al.*, 2010). Anillin was found to interact with F-actin, myosin II, RhoA and Cyk4 (D'Avino *et al.*, 2008; Piekny and Glotzer, 2008). It was suggested that anillin is involved in linking the signals from the mitotic spindles with the equatorial cortex (Gregory *et al.*, 2008).

1.1.2.2.3 *Constriction of the contractile ring*

It has been proposed that the contraction of the contractile ring is achieved by a mechanism similar to muscle contractions (Schroeder, 1972). Consistent with this idea, myosin II filaments were observed in cells at the cleavage furrow during cytokinesis (Yumura *et al.*, 2008; Zhou and Wang, 2008; Vale *et al.*, 2009). Besides its role in generating force to constrict the contractile ring, myosin II was also implicated in the turnover of actin filaments at the equator (Guha *et al.*, 2005; Murthy and Wadsworth, 2005) and thus actin assembly and disassembly had been shown to be important for cytokinesis (Guha *et al.*, 2005; Murthy and Wadsworth, 2005). Our previous study revealed that cytokinesis involves remodelling of cortex associated with cross-linked actin network (Mukhina *et al.*, 2007). These results suggest that cytokinesis requires not only myosin based force but also actin assembly/disassembly and remodelling.

1.1.2.2.4 *Abscission*

The midbody, which connects the two daughter cells and remains connected until the daughter cells are physically separated (Steigemann and Gerlich, 2009; Guizetti and Gerlich, 2010), is composed of a dense array of antiparrallel microtubules and an electron-dense matrix of unknown composition. Proteomics analysis of the midbody revealed the involvement of the components of the membrane fusion machinery, such as syntaxin 2, endobrevin/VAMP-8, and membrane scission machinery components including ESCRT proteins (Skop *et al.*, 2004). Studies on inhibition of the function of these proteins suggested their importance for the abscission (Low

et al., 2003; Hurley and Hanson, 2010; Caballe and Martin-Serrano, 2011; Henne *et al.*, 2011; Morita, 2012). Moreover, membrane trafficking inhibition led to failure of abscission. (Barr and Gruneberg, 2007; Prekeris and Gould, 2008; Schiel and Prekeris, 2010; Neto and Gould, 2011). Recent studies on a microtubule-depolymerising enzyme spastin showed that inhibition of spastin delays the completion of cytokinesis (Connell *et al.*, 2009; Guizetti *et al.*, 2011) and this phenotype can be rescued by microtubule-depolymerising agents (Connell *et al.*, 2009; Guizetti *et al.*, 2011). Moreover, spastin recruitment had been shown to be dependent on ESCRT III (Reid *et al.*, 2005; Yang *et al.*, 2008; Connell *et al.*, 2009). These results suggest that coordinated action of depolymerisation of microtubules with membrane remodelling events might be involved in the abscission process.

1.1.2.3 A question remaining in the cytokinesis field

During past decades, tremendous progress has been made in understanding the mechanism that determines the position of the cleavage furrow where microtubules play a pivotal role in the assembly of the contractile actomyosin ring. However, little is known if actin plays a role in the regulation of the microtubules dynamics and functions during cytokinesis.

Our previous study showed that an actin cross-linking protein α-actinin may be involved in the specification of different populations of microtubules during cytokinesis in mammalian cells (Mukhina et al., 2007; see below for details).

In my thesis project, I have dissected the roles of α-actinin in the regulation of microtubules dynamics and functions during cytokinesis in mammalian cells.

1.2 An actin cross linking protein α-actinin

1.2.1 α-Actinin

α-actinin is an actin crosslinking protein.

Actin cross-linking proteins crosslink F-actin and are responsible for the formation of higher order structures or into meshwork like network of F-actin. F-actin can be organized into parallel or anti-parallel bundles or into meshwork like filaments depending on the type of cross-linking proteins involved in the formation of different structures (Bartles, 2000; Revenu *et al.*, 2004). Parallel and anti-parallel bundles are formed by proteins with two discrete actin-binding domains or multimeric proteins that contain a single actin-binding domain per subunit. However, meshwork like network of actin filaments are formed by ABP with multiple actin binding domains that are separated by flexible spacer domains such as spectrin like repeats which allows more perpendicular arrangements of F-actin (Winder and Ayscough, 2005).

α-actinin is first identified and purified in skeletal muscle (Ebashi and Ebashi 1965). α-actinin has been demonstrated to be an important actin crosslinking protein which localizes to different cellular structures including focal

adhesion, stress fibres in interphase and to the equatorial region during cytokinesis (Otey. C., et al. 2004). Structural studies have shown that α-actinin is composed of three different functional domains (Figure 2). Its N-terminal region is the two calponin homology domain (CH), which is an well characterized as an actin binding domain that is found in many spectrin super-families of proteins. The central region consists of four spectrin like repeats, which are important for forming the anti-parallel rod shape filaments. Apart from its function in forming homo-dimers, spectrin like repeats in α-actinin are thought to provide tensile strength to the rod shaped filamentous structure to α-actinin. Spectrin like repeats also acts as a scaffold for binding to other binding proteins to α-actinin, which may be important for regulating α-actinin's function during different cellular processes. Its C-terminus is composed of two calmodulin-like EF hand motifs that bind to Ca^{2+} and regulate the F-actin binding ability of α-actinin.

α-actinin has been found to be present as an anti-parallel homodimer, with two actin binding domain facing opposite ends of the α-actinin homodimer, which may be important for cross-linking of F-actin. Structural studies of α-actinin have suggested it is both axially curved and twisted (Kristina Djinovic-Carugo. et al., 2002). These properties of the α-actinin allow it be a high-affinity binding site for interacting molecule at the spectrin like repeats. Also, it makes the molecule very elastic, significantly contributing to the stability of the molecule. These peculiar properties of different domains allow it to be amenable to interact with a diverse range of molecules and also to be regulated through different signalling pathways during different cellular processes.

Figure 2: Schematic of α-actinin structure and its major domains.

α-actinin is composed of two actin-binding domains (ABD) in its amino-terminal region (N), four spectrin like repeat in the central region and two EF hand motifs in its carboxy(C) terminal region. α-actinin generally exists as a homodimer.

1.2.2 Roles of α-actinin during cytokinesis

As early as three decades ago it was shown that α-actinin localized to the cleavage furrow region during cytokinesis in chick embryos, sea urching eggs and also in mammalian cells (Fujiwara et al., 1978; Mabuchi et al., 1985; Sanger et al., 1987), suggesting α-actinin may play a role during cytokinesis. Microinjection of antibodies against α-actinin into mammalian cells caused no obvious defects in cytokinesis (Jockusch *et al.*, 1991). In contrast, genetic analysis of fission yeast Ain 1p protein which is an α-actinin like protein was implicated in cytokinesis (Wu et al., 2001). It was shown that, when Ain 1p was deleted it lead to the formation of abnormal actin ring and when it was over expressed it lead to the formation of disorganized or mis-positioned actin rings, suggesting that Ain1p is involved in the formation of equatorial actin ring in fission yeast. Also, deletion or overexpressions of *ain1* in yeast lead to an increase in the number of binucleate cells, suggesting that *ain1* is involved in cytokinesis (Wu et al., 2001). We have previously shown that overexpression of α-actinin inhibits cytokinesis, whereas depletion of α-actinin by RNAi technology induced accelerates cytokinesis and ectopic furrows in mammalian cells (Mukhina et al., 2007). These finding suggest the intriguing possibility that α-actinin may be involved in the regulation of mitotic spindle organization, possibly specifying different microtubule populations.

In order to test this hypothesis I have conducted an in depth analysis of the roles of α-actinin in the specification of different population of microtubules during cytokinesis in mammalian cells using a combination of molecular manipulations and microscope-based technique.

2 Materials and Methods

2.1 Cell Biology

2.1.1 Cell Lines

Table 1: The NRK-52E cell line used in this study

Cell line	NRK-52E
Organism	*Rattus norvegicus* (rat)
Organ	Kidney
Disease	Normal
Growth	Epithelial
Morphology	Adherent
Source	ATCC

Table 2: The HeLa cell line used in this study

Cell line	HeLa
Organism	*Homo sapiens* (Human)
Organ	Cervix
Disease	Adenocarcinoma
Growth	Epithelial
Morphology	Adherent

Source	ATCC

2.1.2 Reagents

2.1.2.1 Antibodies

Table 3: The primary antibodies used in this study along with fixative used and antibody working concentration

Antibody description	Source	Origin	Fixation	Dilution
Anti-α actinin	ImmunoGlobe	Rabbit (polyclonal)	PFA	1:400
Anti-AIM1	Upstate	Mouse (monoclonal)	PFA	1:100
Anti-EB1	BD biotechnologies	Mouse (monoclonal)	PFA	1:300
Anti-MgcracGAP	Genetex	Rabbit (polyclonal)	PFA	1:200
Anti-MKLP1	Santa Cruz Biotechnology	Rabbit (polyclonal)	PFA	1:200
Anti-PRC1	Santa Cruz Biotechnology	Goat (polyclonal)	Methanol	1:200
Anti-α-tubulin	Sigma	Mouse (monoclonal)	PFA/Methanol	1:500

Anti-α-tubulin	Abcam	Rabbit (polyclonal)	PFA	1:200

Table 4: The secondary antibodies used in this study and its working concentration.

Antibody description	Source	Origin	Dilution
Anti-Mouse conjugated with Alexa Fluor 488	Molecular Probes	Goat (polyclonal)	1:200
Anti-Mouse conjugated with Alexa Fluor 543	Molecular Probes	Goat (polyclonal)	1:200
Anti-Rabbit conjugated with Alexa Fluor 488	Molecular Probes	Goat (polyclonal)	1:200
Anti-Rabbit conjugated with Alexa Fluor 543	Molecular Probes	Goat (polyclonal)	1:200
Anti-Goat conjugated with Alexa Fluor 543	Molecular Probes	Rabbit (polyclonal)	1:200

2.1.2.2 Cell culture medium

Dulbecco's modified Eagle medium (DMEM; Sigma) in powder was dissolved in Deionised water and 3.7g/L of sodium bicarbonate was added and the solution pH was adjusted to 6.8 using 1N HCl and filtered using 0.2μm filter and aliquots were stored in an air tight bottles at 4^{o}C. Similarly, Kaighn's modified F12 (F12K; Sigma) in powder was dissolved in Deionised water and 2.5g/L of sodium bicarbonate was added and the solution pH was adjusted to 6.8 using 1N HCl and filtered using 0.2μm filter and aliquots were stored in an airtight bottles at 4^{o}C.

2.1.2.3 Drugs

S-(-) isomer of blebbistatin (Toronto research) stock of 100mM was prepared by dissolving in DMSO and used at a final concentration of 100μM. Cell permeable C3 exoenzyme (Cytoskeleton) was used at final concentration of 2μg/ml. latranculin A (Molecular probes) stock of 1mM was prepared by dissolving in DMSO and used at a final concentration of 1μM. Nocodazole (Sigma) stock of 3.3mM was prepared by dissolving in DMSO and used a final concentration of 0.33μM. G418 (Life Technologies) stock of 50mg/ml was purchased and used at a final concentration of 800μg/ml. DMSO was used a solvent control for all drug treatment experiments. All the stock solutions were stored at -20^{o}C.

Table 5: Drugs used in this study and their mode of action

Name	Mode of action
Blebbistatin	Binds to myosin II ADP-pi binding pocket, there by inhibits myosin II ATPase activity
C3 transferace	Inhibits ADP-ribosylation on asparagines 41 in the effector binding domain of GTPase
Latrunculin	Binds to actin monomers near the nucleotide binding cleft and prevents them from polymerization
Nocodazole	Binds to tubulin dimers and inhibits tubulin polymerization
G418	Blocks polypeptide synthesis by inhibiting the elongation step during translation

2.1.2.4 Solutions

0.05% trypsin:

0.25% trypsin (GIBCO)	10ml
Hank's balanced salt solution (HBBS, GIBCO)	40ml

STE:

NaCl	0.1 M
Tris·Cl(pH 8.0)	10 mM

EDTA (pH 8.0)	1 mM

Cytoskeleton buffer (CB) pH 6.1:

NaCl	137 mM
KCl	5 mM
Na2HPO4	1.1 mM
K2HPO4	0.4 mM
MgCl2	2 mM
EGTA (PH 8.0)	2 mM
PIPES (PH 7.0)	2 mM
Glucose	5.5 mM

HEK (pH 7.5):

HEPES	20 mM
EDTA	1 mM
KCl	50 mM

Lysis buffer10x:

NaCl	5M
Tris	1M
EDTA	0.5M

Phosphate- buffered saline (PBS) pH 7.4:

NaCl	137mM
KCl	2.7mM
Na2HPO4	10 mM
KH2PO4	1.8mM

2.1.2.5 F-actin, DNA markers and microinjection dye

Table 6: F-actin, DNA markers and microinjection dye

Name	Source	Stock concentration	Final concentration
Hoechst 33258	Sigma	10 mg/μl	10 μg/μl
Rhodamine-Phalloidin	Molecular Probes	200 Units/ml	4 Units/ml
Dextran-Fluorescein	Molecular Probes	12.5 mg/ml	2.5 mg/ml

2.1.3 Cell culture conditions

HeLa cells used in this study were cultured in DMEM and NRK cells were cultured in F12K medium which were supplemented with 10% FBS, 1 mM L-glutamine, 100 U/ml penicillin, and 100 μg/ml streptomycin (GIBCO) at 37°C and 5% CO2.

HeLa and NRK cells were maintained in 100 mm or 60 mm polystyrene Petri dishes. Cells were cultured in a custom designed acrylic chamber with glass coverslip in the bottom for all for all live cell imaging and Immuno-fluorescence experiments as described previously (Mckenna and Wang, 1989). Depending on the objectives used for different experiments different thicknesses of glass coverslips were used for best possible optical performance during image acquisition.

Standard cell culture routine was followed for general cell maintenance. In Brief, upon confluence the spent medium in the culture vessels was removed and then briefly rinsed with STE to remove the remaining medium. Then, cells were treated with 0.05% tryspin for a brief interval then incubated for 1-3 minutes, after incubation cells were collected in a pre-warmed culture medium and then seeded into culture dishes.

2.1.4 Trasnfection

Plasmids and siRNA used in this study were transfected using Lipofectamine 2000 reagent (Invitrogen). One day before transfection cells were cultured either in glass bottom cover slip chamber or in culture dishes. On the day of

transfection, cells were briefly rinsed with Opti-MEM (Life technologies) to remove the traces of the complete medium and the transfection mix consisting of either plasmids or siRNA and Lipofectamine reagent were added and incubated for 4 hours. After incubation the transfection mix was replaced by complete medium. The cells were culture for another 24-72 hours post transfection.

2.1.5 Establishment of Stable cell line

Cells stably expressing cherryFP-α-tubulin were generated by transfecting NRK cells with cherryFP-α-tubulin plasmid and culturing them in the presence of 800ug/ml G418 (Life Technologies). Several colonies expressing cherryFP-α-tubulin were isolated using a micromanipulator (Leica) and one of the cell lines expressing cherryFP-α-tubulin from the selection was used in the current study.

2.1.6 Microinjection

Microinjection was performed using a custom drawn glass needles pulled with David-Kopf Model 700 vertical puller and injected using a FemtoJet pressure control system (Eppendorf).

2.1.7 Immunofluorescence

For immunofluorescence experiments, cells were seeded on a glass bottom cover slip chambers. Cells were rinsed twice with prewarmed PBS or CB to remove all the traces of culture medium. They were then treated with either 4% paraformaldehyde (EM Sciences) for 10 minutes in room temperature on a shaker or with ice cold methanol for 15 minutes at -20^{o}C. After fixation cells were washed thrice with PBS or CB at room temperature for 3-5 minutes between each interval. The cells fixed with 4% paraformaldehyde were permeabilized in PBS containing 0.2% Triton X-100 for 5 minutes at room temperature. After permeabilization, both 4% paraformaldehyde and ice cold methanol fixed cells were blocked in 3% BSA (Boehringer Mannheim) in PBS for minimum of 10 minutes at room temperature and then incubated with appropriate primary antibody in a moist chamber for 45-60 minutes at 37^{o}C. After washing three times with 3% BSA in PBS for 3-5 minutes between each interval, the cells were incubated with appropriate secondary antibody in a moist chamber for another 45 minutes at 37^{o}C.

After fluorescent labeling, DNA was stained using 10 ng/ml Hoechst 33258 for 5 minutes at room temperature, then were mounted on a chamber and stored at 4 ^{o}C in PBS.

2.2 Molecular Biology

2.2.1 Plasmid DNA construction

GFP-α-tubulin was obtained from BD Biosciences Clontech. CherryFP-α-tubulin was constructed by replacing the DNA fragment encoding GFP from the GFP-α-tubulin with cherryFP DNA fragment as described (Mukhina *et al.*, 2007). α-actinin-GFP (α-actinin-4-GFP, (AM *et al.*, 2001) was a kind gift from Dr. Carol Otey (University of North Carolina, USA). CherryFP tagged shRNA targeting rat-α-actinin-4 was constructed using that tagged with GFP (SABiosciences). CherryFP coding DNA was amplified using pCMV-cherry vector and the amplified fragment was inserted into rat-α-actinin shRNA (SABiosciences) vector using Xma1 and Age1 restriction sites. The efficiency of knock down of the protein was quantified by staining for α-actinin in rat-α-actinin shRNA cherryFP transfected cells.

2.2.2 siRNA synthesis

siRNA used in this study was prepared using ambion siRNA construction kit. In brief the gene of interest was scanned for AA dinucleotide sequence and the adjacent 3′ 19 nucleotide sequence was chosen for siRNA synthesis. Several primers were designed using the criteria mentioned above along with 8 leader sequence (CCTGTCTC) in the 3′ end of the each primer which is complementary to the T7 promoter primer. For invitro siRNA synthesis the individual sense or antisense primers were incubated with T7 promoter primer along with DNA hybridization buffer, dNTP mix, Klenow reaction buffer and the Exo-Klenow enzyme and incubated for 30 mins at 37^{o}C in a separate reaction mixture. The Klenow extended sense and antisense strands were transcribed using T7 RNA polymerase and the resulting RNA transcripts from

sense and antisense reactions are mixed together to form dsRNA. The purity of dsRNA was confirmed by agarose gel electrophoresis and the concentration of dsRNA was measured using nanodrop.

Table 7: List of siRNA used in this study

Target	Strand	Sequence
Human α-actinin 1	Sense(5′-3′) Antisense(5′-3′)	AAGGTGGAGGAAGAAATCCAG CTGGATTTCTTCCTCCACCTT
Human α-actinin 4	Sense (5′-3′) Antisense(5′-3′)	AAGATGGTATGGACGATGAAC GTTCATCGTCCATACCATCTT
Rat α-actinin 4	Sense(5′-3′) Antisense(5′-3′)	AUGUCUUGGAUGGCGAACCTG CAGGTTCGCCATCCAAGACAT
Human MgcRacGAP1	Sense(5′-3′) Antisense(5′-3′)	AAGACTCTTCTTTGGTGAAGA TCTTCACCAAAGAAGAGTCTT
Control	Sense(5′-3′) Antisense(5′-3′)	AACCTGTCGCTTTCGCGTCTG CAGACGCGAAAGCGACAGGTT

2.2.3 *E.coli* strain growth and maintenance

E.coli XL1 Blue was used for plasmid amplification and maintenance. Bacteria were grown in Luria-Bertani (LB) broth at 37^{o}C

2.2.4 Tranformation of *E.coli*

Heat shock based transformation of *E. coli* was performed by incubating the Heat shock competent *E.coli* along with the plasmid for 45 seconds in a water bath pre-warmed and maintained at 42^{o}C. Immediately after heat shock the bacteria was placed on ice for 2 minutes and then cultured in LB broth for 1 hour at 37^{o}C with vigorous shacking. After the incubation the bacteria was plated on a LB agar with either 100 μg/ml ampicillin or 30 μg/ml kanamycin. Also, in some cases transformation was performed in an electro-competent bacterium using Electroporation using with Biorad$_{TM}$ *E.coli* pulser.

2.3 Biochemistry

2.3.1 Mammalian cell lysis

HeLa cells were rinsed twice with ice-cold PBS to remove all the residual culture medium. Then the cells were covered with a layer of lysis buffer supplemented with complete mini protease inhibitor cocktail (Roche) and Nonidet-40 (NP-40) for 2 minutes on ice. The cells were collected using cell scraper and sonicated thrice for 30 seconds on ice. After sonication the lysates

were collected by spinning the sonicated samples at 10000g for 30 minutes at 4^{o}C. The supernatant was collected and stored at -20^{o}C

2.3.2 Total protein measurement

Total protein concentration in the lysate was estimated using Biorad DC protein assay kit according to the manufacture's recommendation.

2.3.3 SDS-PAGE

Proteins were separated in 10% polyacrylamide gel consisting of 0.5% NN'-methylenebisacrylamide, 0.375 mM Tris-HCL pH 8.8, 0.1% SDS, 0.0075% APS and 0.05% TEMED and the gels were cast with a 1.5 mm spacer. The proteins were diluted in SDS- loading buffer consisting of beta-mercaptoethanol and boiled for 5 mins at 95^{o}C. The proteins were separated in SDS-PAGE using a mini-PROTEAN electrophoresis system (Biorad) using a SDS-running buffer (25 mM Tris, 192 mM glycine and 0.75% SDS) at room temperature.

2.3.4 Immunoblotting and detection

Proteins that were separated using SDS-PAGE were transferred onto a nitrocellulose membrane using Mini Trans-blot electrophoretic Transfer Cell (Bio-Rad) in transfer buffer consisting of (33.7 mM Tris, 256 mM glycine, 20% methanol and 0.01% SDS) at 100 V for 60 minutes at 4^{o}C. After transfer,

the nitrocellulose membrane was blocked with 3% BSA and 0.1% tween-20 in PBS for overnight at 4^{o}C. The membrane was incubated with primary antibody diluted in 3%BSA in PBS for 1 hour at room temperature on a shacking platform and then the membrane was washed thrice with 3%BSA and 0.1% tween-20 in PBS and incubated with secondary antibody diluted in PBS with 0.1% tween-20. After secondary antibody incubation the membrane was washed thrice in 0.1% twee-20 in PBS and the protein was detected using chemiluminescent ECL1 (Amersham) kit as instructed by the manufacturer.

2.3.5 Antibodies

Table 8: List of antibodies used for immunoblotting

Antibody	Source	Origin	Dilution
Anti-α-actinin	Sigma	Mouse (monoclonal)	1:1000
Anti-MgcRacGAP1	Abnova	Mouse (monoclonal)	1:1000
Anti-GAPDH1	IMGENEX	Mouse (monoclonal)	1:2500

Secondary anti-mouse conjugated with peroxidase (HRP; Sigma) was used at a dilution of 1:5000 to detect the protein levels.

2.4 Microscopy techniques

2.4.1 Sample preparation for live cell imaging

For Live cell imaging, cells grown on the custom designed glass bottom cover slip chambers and before imaging cells were washed once with prewarmed complete cell culture medium to remove all floating cells and debris. The glass cover slip chambers with cells were overlaid with a layer of mineral oil (Sigma-Aldrich) to prevent evaporation of the medium during image acquisition.

2.4.2 Sample preparation for Immunofluorescence staining

Immunofluorescence experiments were performed by culturing cells in a glass bottom coverslip chambers. For drug treatment experiments, cells were cultured in a culture medium containing specific drug and incubated for specified amount of time at 37^{o}C in a 5% CO2 incubator. After incubation, cells were rinsed twice in prewarmed PBS or CB to remove all the traces of culture medium and then they were fixed using specified fixative. After fixation cells were washed thrice with PBS or CB at room temperature for 3-5 minutes between each interval, permeabilized in PBS containing 0.2% Triton X-100 for 5 minutes at room temperature. After permeabilization, cells were blocked in 3% BSA (Boehringer Mannheim) in PBS for minimum of 10 minutes at room temperature and then incubated with appropriate primary antibody in a moist chamber for 45-60 minutes at 37^{o}C. After washing three

times with 3% BSA in PBS for 3-5 minutes between each interval, the cells were incubated with appropriate secondary antibody in a moist chamber for 45 minutes at 37^{o}C.

2.4.3 Live cell imaging

Cells cultured in a glass cover slip chambers overlaid with a layer of mineral oil were used for live cell imaging. Live cell imaging was conducted in custom designed incubator maintained at 37^{o}C and 5% CO2 mounted on a Axiovert 200 M inverted microscope (Carl Zeiss) equipped with a 100×, NA1.30, Plan-NEOFLUAR lens and the images were acquired with a cooled charge-coupled device camera (CoolSNAPHQ, Roper Scientific) using MetaView imaging software (Universal Imaging). Alternatively, images were acquired using a Carl Zeiss spinning disc confocal microscope with an incubator maintained at 37^{o}C and 5% CO2 and equipped with a 100x, NA 1.30, Plan-NEOFLUAR lens. Images were acquired with a Hamamatsu Orcr-ERcamera using a MetaView imaging software (Universal imaging).

2.4.4 Immunofluorescence microscopy

The fluorescent signals for immunofluorescene stained samples were acquired using either a LSM 510 Meta confocal microscope system equipped with a 100×, NA 1.4 Plan-Apochromat lens and using Diode laser (405 nm), a Argon multi-line gas laser (458, 477, 488, 514nm), a HeNe gas laser (633 nm) from Carl Zeiss as light source and images were acquired using Photomultiplier

tubes (PMT) detector using LSM image acquisition software (Carl Zeiss). Alternatively, immunofluorescence signals were detected using the Axiovert 200 M inverted microscope equipped with 100×, NA1.30, Plan-NEOFLUAR lens and the images were acquired using cooled charge-coupled device camera (CoolSNAPHQ, Roper Scientific) using MetaView imaging software (Universal Imaging).

2.5 Image analysis

2.5.1 Image processing

Images acquired in Axiovert 200 M inverted microscope and Spinning disc microscope (Carl Zeiss) using Metaview imaging software (Universal Imaging) were processed for Brightness, contrast, crop, and time stamping using either MetaView imaging software or Abode Photoshop CS. Images acquired in LSM 510 Meta confocal microscope system equipped with a 100×, NA 1.4 Plan-Apochromat lens using LSM image acquisition software (Carl Zeiss) were adjusted for brightness, contrast, crop, image merging, stack size selection using LSM image browser (Carl Zeiss) or Image J software.

2.5.2 Quantification of fluorescent signals

Fluorescent intensity signals of sample for analysis were performed using either Image J or MetaView (Universal Imaging). Region of interests were chosen, outlined and the average intensity of signals were measured. An

intensity of the background was also obtained and subtracted with the intensity from the region of interest to obtain a fluorescent intensity of the region of interest. All the measurements were exported into Microsoft excel program and subjected to further analysis.

2.5.3 Quantification of microtubules

Number of microtubules in the cell of interest was analyzed using LSM image browser. In brief, numbers of microtubules were analyzed in only 40% of the total cell volume imaged, which represents the middle region of the total cell volume acquired. For the measurement the start and end of the cell was determined by identifying the fluorescent signals from the F-actin staining and the upper and lower 30% of the cell volume was excluded for the purpose of reducing overestimating the count. In the remaining 40% of the cell volume, the numbers of microtubules in the polar region that were in close proximity to the actin cortex or that were associated with the actin cortex were counted manually. The quantification was logged into a excel file and further analysis was performed using Microsoft excel.

2.5.4 Quantification of EB1 and MKLP1 dots

EB1 dots were counted in the region of interest using LSM image browser. A single confocal plane representing the middle plane of the cell was selected, which was estimated by choosing the plane which showed both the centromeres in the same confocal plane using bright field image. Once the

middle plane was selected the corresponding fluorescent image was chosen and the number of the EB1 in the half spindle of the cell was counted manually. The data was logged in to Microsoft excel file and further analysis was performed.

Alternatively MKLP1 dots were quantified using Image J software. The images of cells of interest were exported as .tiff images and opened using Image J software. Images were first converted into 8 bit format and the region/cell of interest was outline and the rest of the region outside the region of interest was cleared for reducing discrepancy in the analysis. Then the images were converted into black and white image using threshold function and the outline function was used to outline all the dots in the region of interest. The area of dots were measured using measure analyze particle function and the data was exported and further analysis was performed using Microsoft excel.

2.5.5 Kymograhic analysis

Time lapse images were acquired every 2 seconds using spinning disc confocal system (Carl Zeiss). The region of interest was chosen and the kymograph was obtained using metamorph (Universal Imaging).

3. Results

3.1 α-actinin is important for regulation of mitotic spindle organization in mammalian cells

3.1.1 Effects of modulation of α-actinin levels on mitotic spindle organization

To analyze the effects of modulation of α-actinin levels on mitotic spindle organization, NRK cells were transfected with GFP-α-tubulin together with α-actinin-CherryFP or shRNA against α-actinin tagged with CherryFP and were observed under fluorescence microscopy. In control cells expressing GFP-α-tubulin alone, microtubule bundles were found associated with the equatorial cortex during cleavage furrow ingression (12/12). In contrast, in cells expressing GFP-α-tubulin together with α-actinin-CherryFP that showed delayed cytokinesis (Mukhina *et al.*, 2007), equatorial microtubules were poorly bundled. I also noticed that few microtubules were associated with the equatorial cortex (7/25, Figure 3a, Overexpression of α-actinin-CherryFP, arrows). Interestingly, in cells expressing GFP-α-tubulin together with shRNA against α-actinin where ~65% of endogenous α-actinin was depleted (Figure 3b), astral microtubules were associated with the cortex outside the equator and bundled in the ectopic furrow (4/11, Figure 3a, α-actinin shRNA, arrows). All together, these results suggest that α-actinin is involved in the regulation of mitotic spindle organization.

Figure 3: Effects of modulation of α-actinin levels on mitotic spindle organization.

(a) Live-cell images of GFP-α-tubulin in control NRK cells (left) and NRK cells coexpressing α-actinin-CherryFP (middle) or CherryFP-shRNA against α-actinin (right). Microtubule bundles were found associated with the equatorial cortex during cleavage furrow ingression (control, arrows). While in cells expressing GFP-α-tubulin together with α-actinin-CherryFP, equatorial microtubules were poorly bundled (Overexpression of α-actinin-CherryFP, arrows), astral microtubules were associated with the cortex outside the equator and bundled in the ectopic furrow in cells expressing GFP-α-tubulin together with shRNA against α-actinin where ~65% of endogenous α-actinin was depleted (α-actinin shRNA, arrows). Scale bar, 10μm. b) Immunoflourescence images of cells depleted of α-actinin that were stained using antibodies against α-actinin. α-actinin intensity in cells transfected with shRNA against α-actinin was compared with the neighbouring non-transfected cells. c) Graph of quantification of α-actinin fluorescent intensity in shRNA transfected cells compared with neighbouring non-transfected cells.

3.1.2 Effects of depletion of α-actinin on astral microtubules dynamics

A previous report showed that taxol-stabilized microtubules were able to promote furrow ingression outside the equator (Shannon *et al.*, 2005). Thus, we speculated that astral microtubules might be stabilized in cells depleted of α-actinin. Since depletion of α-actinin induced the formation of ectopic furrows even before anaphase onset (Mukhina *et al.*, 2007), we wanted to test if astral microtubules are stabilized during early mitosis in cells depleted of α-actinin. To this end, siRNA against α-actinin was microinjected into NRK cells stably expressing CherryFP-α-tubulin and microtubule dynamics were analyzed using kymograph. In this cell line ~10% of α-tubulin is tagged with CherryFP (Figure 4a and b). Astral microtubules were highly dynamic in control cells expressing CherryFP-α-tubulin at early mitosis (0/13; Figure 4c, Control). Strikingly, astral microtubules became stabilized in early mitotic cells expressing CherryFP-α-tubulin that were microinjected with siRNA against α-actinin (8/23; Figure. 4c, α-actinin siRNA). This suggests that α-actinin is required to maintain the dynamic status of astral microtubules during early mitosis.

To further assess if astral microtubules were stabilized in cells depleted of α-actinin. I also determined the number of EB1 dots in cells depleted of α-actinin. EB1 is a protein strongly associated with the plus end of growing, but not stable, microtubules (Morrison *et al.*, 1998; Tirnauer *et al.*, 2002; Shannon *et al.*, 2005). I found that the number of EB1 dots in cells depleted of α-actinin were significantly reduced (n~4) compared to the control cells (n~9;

Figure 4d and e). These results suggest that astral microtubules are stabilized in cells depleted of α-actinin.

Figure 4: Effects of depletion of α-actinin on astral microtubule dynamics.

(a) Immunofluorescene images of stable cells expressing CherryFP-α-tubulin that were stained for microtubules using antibody against α-tubulin. b) Quantification of the fluorescent intensity of microtubules in control non-transfected cells compared to cells overexpressing CherryFP-α-tubulin. c) Live-cell images of CherryFP-α-tubulin in NRK cells that were injected with either control scrambled siRNA (left, top) or siRNA against α-actinin (left, bottom) during early mitosis. Boxes indicate the regions used for kymographs shown in the right panel. Bar, 10 μm (left). Horizontal bar, 20 s; vertical bar, 2 μm (right). d) Single confocal images of HeLa cells transfected with control scrambled siRNA or siRNA against α-actinin that were stained for DNA (blue) and EB1 (red). Arrowheads indicate representative EB1 comets. Bar, 10 μm. (e) Quantification of the number of EB1 comets except for those along kinetochore microtubules (kMTs) per half cell.

3.1.3 Effects of depletion of α-actinin on microtubule-cortex interactions.

Since, we observed stabilized microtubules in cells depleted of α-actinin. Next, I wanted to examine if astral microtubules become stably associated with the cortex in cells depleted of α-actinin. To this end, HeLa cells were transfected with siRNA against α-actinin (Figure 5a and b) and the number of microtubules associated with the cortex in the half spindle was counted. HeLa cells depleted of α-actinin exhibited abnormal astral microtubule organization (Figure 5c) similar to what I observed in NRK cells depleted of α-actinin (Figure 3a). I detected a significant increase in the number of microtubules associated with the cortex in cells depleted of α-actinin (14.2 ± 0.5; $n = 15$) where the density of F-actin was decreased (Mukhina *et al*., 2007) compared to control cells (9.9 ± 0.4; $n = 16$; $p < 0.0001$) (Figure 5c and d).

Figure 5: Depletion of α-actinin causes stable association of astral microtubules with the actin cortex.

a) Immunoblotting of HeLa cells transfected with siRNA against α-actinin or control scrambled siRNA with anti-actinin antibodies. GAPDH was used as a loading control. b) Live cell imaging of HeLa cells transfected with siRNA against α-actinin. HeLa cells transfected with control scrambled siRNA or siRNA against α-actinin were monitored during cell division by phase contrast microscopy. Time elapsed in mins: seconds after anaphase onset. Scale bar 10 μm. c) Single confocal images of HeLa cells transfected with control scrambled siRNA or siRNA against α-actinin that were stained for DNA (blue), F-actin (red), and microtubules (green). Scale bar, 10 μm. On the right, the indicated regions in control cells and cells depleted of α-actinin are shown at higher magnification. Bar, 1 μm. d) Quantification of microtubule-actin cortex associations in HeLa cells transfected with control scrambled siRNA or siRNA against α-actinin.

3.1.4 Effects of depolymerization of F-actin and RhoA inhibition on microtubule-actin cortex interaction

As earlier we had shown that depletion of α-actinin stabilization of astral microtubules and also caused reduction in the overall F-actin density in the cells. I next examined if reduction of F-actin density by either inhibiting actin polymerization or RhoA inhibition causes stable association of microtubules with actin cortex as seen in cells depleted of α-actinin. To this end, I treated cells with either latrunculin A, an inhibitor of actin polymerization, or cell permeable C3, a RhoA inhibitor and the number of microtubules associated with the cortex in the half spindle was counted. Treatment of cells with latrunculin A, did not promote stable microtubule-cortex associations (Figure 6a). Similarly, treatment of cells with a cell permeable Rho inhibitor C3 enzyme caused a decrease in F-actin density but no significant increase in the number of microtubules associated with the cortex was observed (7.3 ± 0.2; $n = 11$) as compared to DMSO-treated cells (7.1 ± 0.4; $n = 10$) (Figure 6b and c). These results suggest that α-actinin-dependent cortical F-actin integrity is required to prevent stable microtubule-cortex association.

Figure 6: Effects of depolymerization of F-actin and RhoA inhibition on microtubule-cortex interaction

a) Single confocal images of HeLa cells treated with DMSO or latrunculin A that were stained for F-actin (red), DNA (blue) and microtubules (green). Scale bar, 10 μm. b) Single confocal images of HeLa cells treated with DMSO or cell permeable C3 that were stained for DNA (blue), F-actin (red), and microtubules (green). Bar, 10 μm. (c) Quantification of microtubule-actin cortex associations in HeLa cells treated with DMSO or cell permeable C3.

3.1.5 Effects of inhibition of myosin II activity on microtubule-cortex interactions in cells depleted of α-actinin.

Previously, it has been shown that ectopic furrow formation in cells depleted of α-actinin requires myosin II activity (Mukhina *et al,* 2007), I wanted to determine if stable microtubule-cortex associations induced by depletion of α-actinin requires myosin II activity. To this end, first I checked the effect of blebbistatin a specific inhibitor of myosin II ATPase activity (Straight *et al.*, 2003) treatment on mitotic spindle organization of normal wild type HeLa cells (Figure 7a) and I also treated cells depleted of α-actinin with blebbistatin and the number of microtubules associated with the cortex in the half spindle was counted. The number of microtubules associated with the cortex (8.2 ± 0.3; n = 13) in cells deplted of α-actinin was significantly less compared to cells depleted of α-actinin that were treated with DMSO (12.5 ± 0.6; n = 12; $p < 0.0001$) (Figure 7b and c), suggesting that α-actinin is required to prevent stable microtubule-cortex associations through suppressing myosin-based cortical contractility.

Figure 7: Effects of inhibition of myosin II activity on microtubule-cortex interactions in cells depleted of α-actinin.

(a) Single confocal image of wild type HeLa cells treated with DMSO or blebbistatin and were stained for microtubules (green), MKLP1 (red) and DNA (blue). Scale bar 10 μm. Note that cells treated with blebbistatin in wild type HeLa cells causes no apparent effects on microtubule organization. b) Single confocal images of HeLa cells transfected with siRNA against α-actinin that were treated with DMSO or blebbistatin and were then stained for DNA (blue), F-actin (red), and microtubules (green). Scale bar, 10 μm. (c) Quantification of microtubule-actin cortex associations in HeLa cells transfected with siRNA against α-actinin that were treated with DMSO or blebbistatin.

3.2 Roles of α-actinin in localization of microtubule-associated cytokinetic regulators during cell division

3.2.1 Depletion of α-actinin causes aberrant localization of centralspindlin but not PRC1 and aurora B to the tips of astral microtubules

Earlier we showed that depletion of alpha-actinin cause stabilization of astral microtubule and it has been reported that stabilization of microtubules requires several cytokinetic regulators. I wanted to determine if microtubule-associated cytokinetic regulators are involved in stable microtubule-cortex associations induced by depletion of α-actinin. To test this, I first analyzed if centralspindlin, composed of MKLP1 and MgcRacGAP, is involved in stable microtubule-cortex associations induced by depletion of α-actinin. Strikingly, I found that small dot-like structures of MKLP1 were localized at the tips of astral microtubules in close proximity to the cortex in cells depleted of α-actinin (7/19; Figure 8a, α-actinin siRNA), whereas it was faintly localized to the kinetochore microtubules in control cells (0/14; Figure 8a, control; (Sellitto and Kuriyama, 1988). Similar localization patterns of MgcRacGAP were detected in cells depleted of α-actinin (5/16, Figure 8b, α-actinin siRNA).

In contrast to centralspindlin, both aurora B, a component of CPC, and PRC1 were rarely detected at the tips of astral microtubules in cells depleted of α-actinin (n = 17 for aurora B, Fig 8c, n = 11 for PRC1; Figure 8d). These results suggest that α-actinin plays an important role in preventing aberrant

localization of centralspindlin to the tips of astral microtubules, which causes stable microtubule-cortex association during early mitosis.

Figure 8: Depletion of α-actinin causes aberrant recruitment of centralspindlin but neither PRC nor aurora B to astral microtubules during early mitosis.

(a,,b,c,) Z-stack confocal images of HeLa cells transfected with control scrambled siRNA or siRNA against α-actinin that were stained for microtubules (green), MKLP1 (a, red), MgcRacGAP (b, red), or aurora B (c, red) and DNA (blue). Scale bar 10 μm (d) Single confocal images of HeLa cells transfected with control scrambled siRNA or siRNA against α-actinin that were stained for microtubules (green), PRC1 (red) and DNA. Scale bar, 10 μm.

3.2.2 Centralspindlin is indeed associated with astral microtubules in cells depleted of α-actinin during early mitosis

Since, we observed ectopic localization of cytokinetic regulators including MKLP1to the tips of astral microtubule. I wanted to demonstrate clearly that they are indeed localized to the tips of astral microtubule and not just localized in the cytoplasm near the microtubule tips. To test this, I treated cells depleted of α-actinin and wild type HeLa cells with nocodazole and stained for microtubules. In cells depleted of α-actinin or non-transfected wild type cells that were treated with nocodazole, we rarely observed MKLP1 near the actin cortex (0/24; Figure 9a and b, nocodazole treated). In contrast, in cells depleted of α-actinin that were treated with DMSO, dot-like structures of MKLP1 were detected near the cortex. These results suggest that centralspindlin indeed becomes localized to the tip of astral microtubules in cells depleted of α-actinin.

Figure 9: Centralspindlin is indeed associated with microtubules in cells depleted of α-actinin during early mitosis

a) HeLa cells transfected with siRNA against α-actinin were treated with DMSO, and microtubule depolymerising agent, nocodazaole. The cells were fixed and stained for microtubules (green), MKLP1 (red), and DNA (blue). Scale bar, 10μm. b) Single confocal images of wild type HeLa cells treated with DMSO and nocadazole were stained for microtubules (green), MKLP1(red) and DNA (blue). Scale bar, 10μm.

3.2.3 Aberrant localization of centralspindlin induced by depletion of α-actinin is dependent on myosin II activity

As we had demonstrated that α-actinin is required to prevent stable microtubule-cortex associations through suppressing myosin-based cortical contractility. I next asked if aberrant localization of MKLP1 induced by depletion of α-actinin is dependent on myosin II activity. To test this possibility, I treated cells depleted of α-actinin with a specific inhibitor of myosin II ATPase activity, blebbistatin (Straight *et al.*, 2003) and stained them for MKLP1. In cells depleted of α-actinin or wild type cells that were treated with blebbistatin, MKLP1 was rarely detected at the tips of microtubules near the actin-cortex (0/10; Figure 10 and b, blebbistatin). In contrast, in cells depleted of α-actinin or wild type that were treated with DMSO, MKLP1 was found localized at the tips of microtubules near the actin-cortex (Figure 10a and b, DMSO). These results suggest that α-actinin prevents MKLP1 from localizing to the tips of astral microtubules through suppressing myosin-based cortical contractility.

Figure 10: Inhibition of myosin II activity in cells depleted of α-actinin prevents MKLP1 from localizing to the tips of astral microtubules.

a) Z-stack confocal images of HeLa cells transfected with siRNA against α-actinin that were treated with DMSO or blebbistatin and were stained for microtubules (green), MKLP1 (red) and DNA (blue). Scale bar, 10 μm. b) Z-stack confocal images of wild type HeLa cells that were treated with DMSO or blebbistatin were stained for microtubules (green), MKLP1 (red) and DNA (blue). Scale bar, 10 μm.

3.2.4 Stable microtubule-actin cortex interactions induced by depletion of α-actinin is caused by mislocalization of centralspindlin to astral microtubules

Since α-actinin depletion causes stabilisation of astral microtubules and also mislocalization of cytokinetic regulator complex centralspindlin, I wanted to test which one these process is the effected by α-actinin depletion. To understand this I hypothesized that depletion of α-actinin caused stable microtubule-actin cortex interactions through recruiting centralspindlin to astral microtubules. To test this hypothesis, both α-actinin and MgcRacGAP were depleted from HeLa cells and these cells were stained for microtubules and F-actin and the number of microtubules that were in close proximity to the actin cortex was counted. Strikingly, I found that in cells depleted of both MgcRacGAP1 and α-actinin (Figure 11a and b), astral microtubules failed to stably associate with the actin cortex (n=16, Figure 11c) and the number of microtubules found in close proximity to the actin cortex were significantly reduced (Figure 11d). In contrast, cells depleted of α-actinin alone astral microtubules were found stably associated with the actin-cortex (Figure 11c and d, α-actinin siRNA). Taken together, these results suggest that α-actinin is required to maintain the dynamic status of astral microtubules by preventing the recruitment of centralspindlin to astral microtubules.

Figure 11: Effect of double depletion of α-actinin and MgcRacGAP on astral microtubule actin-cortex interaction.

(a) Immunoblotting of HeLa cells transfected with control scrambled siRNA, siRNA against α-actinin, or siRNA against α-actinin and MgcRacGAP with anti-actinin antibodies. b) Immunoblotting of HeLa cells transfected with control scrambled siRNA, siRNA against α-actinin, or siRNA against α-actinin and MgcRacGAP with anti-MgcRacGAP antibodies. In both a and b GAPDH was used as a loading control. c) Single confocal images of HeLa cells transfected with control scrambled siRNA, siRNA against α-actinin, or siRNA against α-actinin and MgcRacGAP that were stained for DNA (blue), F-actin (red), and microtubules (green). Scale bar, 10 μm. (d) Quantification of microtubule-actin cortex associations in HeLa cells transfected with control scrambled siRNA, siRNA against α-actinin, or siRNA against α-actinin and MgcRacGAP.

3.2.5 Depletion of α-actinin causes aberrant localization of centralspindlin components MKLP1 and MgcRacGAP to the polar astral microtubules during late mitosis.

Next I examined the effects of depletion of α-actinin on microtubule organization and localization of centralspindlin during late mitosis**.** I found that a subset of astral microtubules was elongated to the equatorial cortex, while well-organized midzone microtubules were formed in control cells (Figure 12a, Microtubules, control). In contrast, in cells depleted of α-actinin, astral microtubules were extensively elongated toward the entire cortex and midzone microtubules were poorly organized (Figure 12a and b, Microtubules, α-actinin siRNA).

Both MKLP1 and MgcRacGAP were concentrated to the midzone in control cells, whereas they were detected throughout entire cortex with dot-like structures and failed to fully concentrate in the midzone in cells depleted of α-actinin (3/8; Figure 12a, a MKLP1 and 6/19; 12b, MgcRacGAP). These results suggest that aberrant recruitment of centralspindlin to polar astral microtubules induced by depletion of α-actinin leads to impaired formation of midzone microtubules.

Figure 12: Aberrant microtubule organization and localization of centralspindlin in cells depleted of α-actinin during late mitosis.

(a, b) Z-stack confocal images of HeLa cells transfected with control scrambled siRNA or siRNA against α-actinin that were stained for microtubules (green), MKLP1 (a, red) or MgcRacGAP (b, red) and DNA (blue). Scale bar, 10 μm.

3.2.6 MKLP1 forms larger clusters outside the equatorial region in cells depleted of α-actinin.

As we showed earlier that depletion of α-actinin cause mislocalization of MKLP1 during both early and late mitosis and it has been suggested that clustering of centralspindlin promotes its association with microtubules plus ends. I wanted to test if there is any change in size of MKLP1 dot during early and late mitosis in cells depleted of α-actinin. To test this, I quantified the size of dot-like structures of MKLP1 that were localized throughout the cell at metaphase and outside the equator at anaphase in cells depleted of α-actinin (Figure 13a and b). In control cells, more than 90% of the MKLP1 dots were ≤ 3.6×10^{-3} μm^2 in both metaphase and anaphase cells (Figure 13d). In contrast, more than 25% and 32% of the MKLP1 dots were > 3.6×10^{-3} μm^2 in cells depleted of α-actinin at metaphase and anaphase, respectively (Figure 13d) . Moreover, in cells depleted of α-actinin at anaphase, ~55% of the dots that showed > 3.6×10^{-3} μm^2 were > 7.2×10^{-3} μm^2 (Figure 13c). A recent study demonstrated that centralspindlin formed clusters through Zen-4, an MKLP1 homolog in nematode (Hutterer *et al.*, 2009). These results suggest that centralspindlin forms larger clusters after cells enter anaphase and that clustering may be at least partly involved in the α-actinin-mediated mechanism.

Figure 13: Quantification of the size of MKLP1 dots in early and late mitosis.

Quantification of the MKLP1 dots in HeLa cells transfected with control scrambled siRNA or siRNA against α-actinin at metaphase (a) and anaphase (b). In anaphase cells the MKLP1 dots that were localized outside the equatorial region were analyzed. Scale bar, 10 μm. A graph in (c) shows the percentage of the small (3.6 - 7.2 x 10^{-3} μm^2) and the large sizes (>7.2 x 10^{-3} μm^2) of the MKLP1 dots in HeLa cells transfected with siRNA against α-actinin at metaphase and anaphase. d) graph shows the percentage of total dots counted in metaphase and anaphase. Red arrows in (a) and (b) indicate representative large MKLP1 dots.

3.2.7 Aberrant localization of centralspindlin induced by α-actinin depletion is dependent on myosin II activity during late mitosis.

Next, I wanted to test if aberrant localization of MKLP1 and microtubule organization in cells depleted of α-actinin is dependent on myosin II activity during late mitosis. To test this, I treated cells depleted of α-actinin with blebbistatin and imaged using confocal microscopy. I observed, no apparent defects in microtubule organization as well as MKLP1 localization were detected (0/9; Figure 14a). However in wild type cells treated with blebbistatin and DMSO, MKLP1 failed to accumulate the equatorial cortex compared to DMSO treated cells, where MKLP 1 was found on the equatorial cortex (Figure 14b, white arrows). This result suggests that aberrant localization of centralspindlin induced by α-actinin is dependent on myosin II activity during late mitosis.

Figure 14: Aberrant localization of centralspindlin is dependent on myosin II activity in cells depleted of α-actinin during late mitosis.

a) Single confocal images of HeLa cells transfected with siRNA against α-actinin that were treated with DMSO or blebbistatin and were then stained for microtubules (green), MKLP1 (red) and DNA (blue). Scale bar, 10 μm. b) Single confocal images of wild type HeLa cells treated with DMSO or blebbistatin and were then stained for microtubules (green), MKLP1 (red) and DNA (blue). Scale bar, 10 μm.

3.2.8 Depletion of α-actinin causes a failure of complete relocation of aurora B from chromosomes to midzone microtubules during late mitosis.

Previous studies showed that midzone microtubules are required for midzone localization of aurora B (Murata-Hori and Wang, 2002; Fuller *et al.*, 2008). Thus, I examined if aurora B localization is affected in cells depleted of α-actinin. In control cells that were treated with control scrambled siRNA (12/12; Figure 15, control), aurora B was localized in the equatorial region. In contrast, in cells depleted of α-actinin, a fraction of aurora B remained associated with the chromosomes (4/13; Figure 15, α-actinin siRNA). This result suggests that midzone microtubules are not properly assembled most likely due to the lack of non-microtubule-associated centralspindlin that is required for their assembly

Figure 15: Aurora B localization in cells depleted of α-actinin during late mitosis

Single confocal images of HeLa cells transfected with control scrambled siRNA or siRNA against α-actinin that were stained for microtubules (green), aurora B (red), and DNA (blue). A fraction of aurora B remained associated with chromosomes. Scale bar, 10 μm.

Discussion

Our previous study suggested that tight regulation of cortical actin mediated by α-actinin is essential for cytokinesis (Mukhina *et al*., 2007). In this study, we showed that depletion of α-actinin caused accelerated cytokinesis and ectopic furrowing, suggesting that α-actinin plays important roles in the regulation of the speed of cytokinesis and the position of the cleavage furrow.

In this study, I studied how α-actinin regulates the position of the cleavage furrow by analyzing its roles in the regulation of microtubule dynamics/organization.

Roles of astral and midzone microtubules in the cleavage furrow positioning in mammalian cells

There is a longstanding paradox in the roles of microtubules in the determination of the cleavage furrow position. Pioneering studies showed that astral microtubules are responsible for the cleavage furrow positioning in sea urchin embryos (Rappaport, 1961), whereas midzone but not astral microtubules are important to determine the furrow position in mammalian tissue cultured cells (Cao and Wang, 1996).

Previous studies with *C. elegans* embryos suggest that both astral and midzone microtubules can position the cleavage furrow (Bringmann and Hyman, 2005). Our observations suggest that in mammalian cells both astral and midzone microtubules are also able to induce furrow ingression when they interact with

centralspindlin. However, in *C. elegans* embryo, astral microtubules positioned the cleavage furrow in the absence of a kinesin-6 Zen-4 (Bringmann and Hyman, 2005). Thus, although both astral and midzone microtubules could position the cleavage furrow regardless of cell type, the molecular mechanism underlying positioning of the cleavage furrow might be cell type-dependent.

My results also suggest that centraspindlin but not PRC1 nor aurora B is a key player in the determination of the cleavage furrow positioning. It has been suggested that Aurora B may be a signal for cytokinesis (Murata-Hori *et al.*, 2002; Hu *et al.*, 2008). However, aurora B was rarely observed at the tips of polar astral microtubules in cells depleted of α-actinin (Figure 8). Although I cannot rule out the possibility that undetectable level of aurora B might be recruited to them (Murata-Hori and Wang, 2002), the present study suggests that centralspindlin, most probably together with the RhoGEF Ect2 (Yüce *et al.*, 2005; Zhao and Fang, 2005; Chalamalasetty *et al.*, 2006; Kamijo *et al.*, 2006; Nishimura and Yonemura, 2006), could be sufficient for induction of furrowing likely through regulating Rho pathway (see also below). Interestingly, in C. elegans embryos where either of a component of CPC or centralspindlin was mutated, the rate of the constriction of the cleavage furrow was similar between these embryos, suggesting that CPC and centralspindlin may function in furrow ingression independently (Lewellyn *et al.*, 2011).

Roles of alpha-actinin in the association of centralspindlin with microtubules

I showed that depletion of α-actinin caused aberrant recruitment of centralspindlin to astral microtubules, making them 'equatorial'-like microtubules (Figure 8a and 12a). How does depletion of α-actinin induce association of centralspindlin with astral microtubules? My results suggest that increased cortical contractility throughout the cell by depletion of α-actinin may promote transport of the cytoplasmic pool of centralspindlin toward these microtubules. Centralspindlin is known to form clusters and clustering significantly contributes to its microtubule bundling activity (Mishima *et al.*, 2002). It was also shown that the clustering contributes to the accumulation of centralspindlin to the plus ends of microtubules (Hutterer *et al.*, 2009). My results suggest that centralspindlin forms larger clusters after cells enter anaphase and that clustering may be at least partly involved in the α-actinin-mediated mechanism.

Regulation of the cleavage furrow ingression by midzone microtubules

Cytokinesis was accelerated in cells depleted of α-actinin (Mukhina *et al*., 2007) where midzone microtubules are not properly formed (Figure 12a and b), suggesting that functional midzone microtubules are dispensable for cytokinesis when astral microtubules are associated with centralspindlin and that midzone microtubules likely control the speed of furrow ingression through coordinating microtubule bundling with cortical contractions. A

previous study using *C.elegans* embroyos suggests that reduced microtubule density triggers furrow initiation (Dechant and Glotzer, 2003). A theoretical model suggests that a local minimum of microtubule density is important for triggering the cleavage furrow formation (Yoshigaki, 1999). These results also suggest that the density of microtubules influences furrow ingression.

Roles of microtubules in inhibition of furrow ingression outside the equator

It has been suggested that stabilized microtubules induce furrow ingression whereas dynamic astral microtubules inhibit furrow ingression in mammalian cells(Canman *et al.*, 2003). Taxol treated microtubules could induce furrow ingression outside the equator (Shannon *et al*., 2005), indicating that stabilized microtubules are able to induce furrow ingression. In other words, maintenance of dynamic state of microtubules is important to inhibit furrow ingression.

Inhibition of the activity of a CPC component aurora B caused abnormal elongation and bundling of astral microtubules and induced initiation but not completion of ectopic furrowing (Miyauchi *et al.*, 2007). However, a centralspindlin component MKLP1 was not detected in these bundled microtubules (Miyauchi *et al.*, 2007). Therefore, it is possible that induction of ectopic furrowing in cells where aurora B activity was inhibited could be induced by the different mechanism from what is seen at the equator in cytokinesis in normal cells and ectopic furrow in α-actinin depleted cells

where the furrowing is completed. Taxol-treated microtubules, that were not associated with CPC, were able to induce the initiation but not completion of furrowing outside the equator (Shannon *et al*., 2005). These observations suggest that inhibition of the stabilization of microtubules is important to prevent ectopic furrowing and thus faithful cytokinesis. It is unclear how stabilized microtubules that are not associated with cytokinetic regulators induce furrowing. They may be able to deliver the positive signals to cell cortex for furrowing or stimulate cortical contraction by unknown mechanisms,

Roles of alpha-actinin in the regulation of the actin cell cortex during cytokinesis

Cell cortex interacts with and responds to a range of physical and chemical factors. Cells are known to undergo drastic changes in the physical stiffness in a cell cycle-dependent manner (Kunda and Baum, 2009). At the cell cortex, F-actin interacts with actin-crosslinking proteins and forms a gel-like network. Overexpression of α-actinin increased cortical rigidity during mitosis (Mukhina *et al*., 2007). In cells depleted of α-actinin, I observed the reduction in the density of F-actin throughout the cell cortex and the formation of ectopic furrows (Figure 5). This result suggests that maintenance of cortical rigidity by α-actinin outside the equator may be important to inhibit furrow ingression.

Regulation of equatorial microtubules by α-actinin during cytokinesis

How does α-actinin regulate microtubules at the equator during cytokinesis in normal condition? Several studies have revealed that centralspindlin accumulates at the tips of microtubules at the cortex of the midzone (Nishimura and Yonemura, 2006; D'Avino *et al.*, 2008; Hu *et al.*, 2008). After anaphase onset, α-actinin accumulates at the equator in an actin-dependent manner (Low *et al.*, 2010). α-actinin is highly dynamic at the equatorial region compared to the polar regions (Mukhina *et al*., 2007). The difference of its dynamics between these regions likely reflects the difference in the F-actin crosslinking status and thus cortical contractility. It is possible that cortical contractility is higher at the equatorial region than other regions even before furrow initiation. High levels of cortical contractility at the equatorial region likely promote recruitment of centralspindlin to microtubules and lead to their stable association with the cortex at this region. This possibility is supported by the evidence that MKLP1 was rarely detected at the equatorial cortex before furrow initiation when cells were treated with blebbistatin (Figures 14). Stabilized equatorial microtubules activate Rho, leading to increased myosin II activity through regulating its downstream effectors (Piekny *et al.*, 2005). Increased myosin II activity would promote release of α-actinin from the equatorial region (Mukhina *et al*., 2007;Reichl and Robinson, 2007), leading to an increase in cortical contractility and thus allowing contraction to proceed. Increased cortical contractility then promotes recruitment of centralspindlin to astral microtubules at the equatorial region, creating positive feedback loop in promoting cytokinesis (Figure 16).

Our observations suggest that the different F-actin crosslinking status by α-actinin between equatorial and polar regions is critical for the formation of different populations of microtubules during cell division. Such difference is likely due to different myosin II activity and/or actin dynamics/organization between these regions. Previous studies have demonstrated that actin is highly dynamic at the equatorial region (Pelham and Chang, 2002; Murthy and Wadsworth, 2005), suggesting that the dynamic state of actin is important for that of α-actinin. Thus, assembly of dynamic F-actin may be crucial not only for proper cortical ingression (O'Connell *et al.*, 2001) but for local stabilization of microtubules at the equator during cytokinesis.

Conclusion

Cytokinesis is a complex process that is regulated by microtubules and actin cytoskeleton. While microtubules are responsible for the determination of the cleavage furrow position, F-actin plays an essential role in pinching off the cell. Recent advances in genetics, proteomics, chemical screening, and microscope imaging techniques have made significant contributions to understanding the molecular mechanism underlying the determination of the cleavage furrow position where actin assembles. However, little is known if and how actin regulates microtubules during cytokinesis. In this thesis, I found that an actin cross-linking protein α-actinin plays a previously unappreciated role in the regulation of mitotic spindle organization and microtubule dynamics. As seen in other cellular processes, my findings suggest that microtubules and actin do crosstalk in cytokinesis. Future experiments should address if other microtubule-associated cytokinetic components such as Kif4 and Plk1 are regulated by alpha-actinin.

Figure 16: Proposed model for the feedback loop mechanism

From my experiments data, I propose that increased myosin II activity would promote release of α-actinin from the equatorial region (Mukhina et al., 2007; Reichl and Robinson, 2009), leading to an increase in cortical contractility and thus allowing contraction to proceed. Increased cortical contractility then promotes recruitment of centralspindlin to astral microtubules at the equatorial region, creating positive feedback loop in promoting cytokinesis.

Future directions:

We have shown that depletion of α-actinin cause stabilization of astral microtubule even before anaphase onset and also mislocalization of cytokinetic regulators to the tips of astral microtubules; however, how α-actinin depletion causes these changes is still not clearly understood. So, in future using a combination of micromanipulation combined with advanced microscope based technique it will be interesting to study the effect of local depletion or inactivation of α-actinin on microtubules organization and also of cytokinetic regulators as seen in cells depleted of α-actinin. This can provide a more direct evidence for the role of of α-actinin on microtubule organization during cytokinesis in mammalian.

Also, as there is a changes in crosslinking status of F-actin in different region of cells during mitosis, it will be interesting to effect of spatio- temporally changes in crosslinking status of F-actin on microtubule organization. To test this, combination of advanced microscopy along with micromanipulation techniques could be utilized to study the effect of different crosslinking status of F-actin on microtubule organization.

As a-actinin localization changes dramatically from focal adhesion and stress fibers in interphase to actin cortex and to the equatorial region during cytokinesis, it will be interesting to study the signalling that mediate these changes in α-actinin localization during different cell cycle stages. To test this, I would like to create different α-actinin point mutants which are defective in post translational including phosphorylation defective mutant and ask how these mutants behave during different stages of cell cycle.

5 References

Alsop, G.B., and Zhang, D. (2003). Microtubules are the only structural constituent of the spindle apparatus required for induction of cell cleavage. J Cell Biol *162*, 383-390.

AM, G., C, O., M, E., and CR., J. (2001). Interactions of a hemidesmosome component and actininfamily members. . J Cell Sci *114*.

Amano, M., Ito, M., Kimura, K., Fukata, Y., Chihara, K., Nakano, T., Matsuura, Y., and Kaibuchi, K. (1996). Phosphorylation and activation of myosin by Rho-associated kinase (Rho-kinase). J Biol Chem *271*, 20246-20249.

Assaad, F.F. (2001). Plant cytokinesis. Exploring the links. Plant Physiol *126*, 509-516.

Barr, F.A., and Gruneberg, U. (2007). Cytokinesis: placing and making the final cut. Cell *131*, 847-860.

Bartles, J.R. (2000). Parallel actin bundles and their multiple actin-bundling proteins. Curr Opin Cell Biol *12*, 72-78.

Beggs, A.H., Byers, T.J., Knoll, J.H.M., Boyce, F.M., Bruns, G.A.P., and KunkelS, L.M. (1992). Cloning and Characterization oTf wo Human Skeletal Muscle alpha-Actinin Genes Located on Chromosomes 1 and 11. The Journal of Biological Chemistry *267*, 8.

Bender, A, and Pringle, J.R. (1989). Multicopy suppression of the cdc24 budding defect in yeast by CDC42 and three newly identified genes including the ras-related gene RSRI. Proc. Natl. Acad. Sci. USA *89*, 5.

Bi, E. (2001). Cytokinesis in budding yeast: The relationship between actomyosin ring function and septum formation. Cell Structure and Function *26*, 9.

Bieling, P., Telley, I.A., and Surrey, T. (2010). A minimal midzone protein module controls formation and length of antiparallel microtubule overlaps. Cell *142*, 420-432.

Biron, D., Alvarez-Lacalle, E., Tlusty, T., and Moses, E. (2005). Molecular model of the contractile ring. Phys Rev Lett *95*, 098102.

Bringmann, H., and Hyman, A.A. (2005). A cytokinesis furrow is positioned by two consecutive signals. Nature *436*, 731-734.

Burridge, K., and Feramisco, J.R. (1981). Non-muscle alpha actinins are calcium-sensitive actin-binding proteins. Nature *294*, 565-567.

Burtnick, L.D., Urosev, D., Irobi, E., Narayan, K., and Robinson, R.C. (2004). Structure of the N-terminal half of gelsolin bound to actin: roles in severing, apoptosis and FAF. EMBO J *23*, 2713-2722.

Bähler, J., Steever, A.B., Wheatley, S., Wang, Y., Pringle, J.R., Gould, K.L., and McCollum, D. (1998). Role of polo kinase and Mid1p in determining the site of cell division in fission yeast. J Cell Biol *143*, 1603-1616.

Caballe, A., and Martin-Serrano, J. (2011). ESCRT machinery and cytokinesis: the road to daughter cell separation. Traffic *12*, 1318-1326.

Calvert, M.E., Wright, G.D., Leong, F.Y., Chiam, K.H., Chen, Y., Jedd, G., and Balasubramanian, M.K. (2011). Myosin concentration underlies cell size-dependent scalability of actomyosin ring constriction. J Cell Biol *195*, 799-813.

Canman, J.C., Cameron, L.A., Maddox, P.S., Straight, A., Tirnauer, J.S., Mitchison, T.J., Fang, G., Kapoor, T.M., and Salmon, E.D. (2003). Determining the position of the cell division plane. Nature *424*, 1074-1078.

Cao, L.G., and Wang, Y.L. (1996). Signals from the spindle midzone are required for the stimulation of cytokinesis in cultured epithelial cells. Mol Biol Cell *7*, 225-232.

Carvalho, A., Desai, A., and Oegema, K. (2009). Structural memory in the contractile ring makes the duration of cytokinesis independent of cell size. Cell *137*, 926-937.

Casamayor, A., and Snyder, M. (2002). Bud-site selection and cell polarity in budding yeast. Curr Opin Microbiol *5*, 179-186.

Castrillon, D.H., and Wasserman, S.A. (1994). Diaphanous is required for cytokinesis in Drosophila and shares domains of similarity with the products of the limb deformity gene. Development *120*, 3367-3377.

Caviston, J.P., Longtine, M., Pringle, J.R., and Bi, E. (2003). The role of Cdc42p GTPase-activating proteins in assembly of the septin ring in yeast. Mol Biol Cell *14*, 4051-4066.

Chalamalasetty, R.B., Hümmer, S., Nigg, E.A., and Silljé, H.H. (2006). Influence of human Ect2 depletion and overexpression on cleavage furrow formation and abscission. J Cell Sci *119*, 3008-3019.

Chant, J. (1999). Cell polarity in yeast. Annu Rev Cell Dev Biol *15*, 365-391.

Chant, J., Corrado, K., Pringle, J.R., and Herskowitz, I. (1991). Yeast BUDS, Encoding a Putative GDP-GTP Exchange Factor, Is Necessary for Bud Site Selection and Interacts with Bud Formation Gene BEAM. Cell *65*, 12.

Cheng, H., Sugiura, R., Wu, W., Fujita, M., Lu, Y., Sio, S.O., Kawai, R., Takegawa, K., Shuntoh, H., and Kuno, T. (2002). Role of the Rab GTP-binding protein Ypt3 in the fission yeast exocytic pathway and its connection to calcineurin function. Mol Biol Cell *13*, 2963-2976.

Connell, J.W., Lindon, C., Luzio, J.P., and Reid, E. (2009). Spastin couples microtubule severing to membrane traffic in completion of cytokinesis and secretion. Traffic *10*, 42-56.

D'Avino, P.P., Takeda, T., Capalbo, L., Zhang, W., Lilley, K.S., Laue, E.D., and Glover, D.M. (2008). Interaction between Anillin and RacGAP50C connects the actomyosin contractile ring with spindle microtubules at the cell division site. J Cell Sci *121*, 1151-1158.

Dechant, R., and Glotzer, M. (2003). Centrosome separation and central spindle assembly act in redundant pathways that regulate microtubule density and trigger cleavage furrow formation. Dev Cell *4*, 333-344.

Djinovic-Carugo, K., Young, P., Gautel, M., and Saraste, M. (1999). Structure of the alpha-Actinin Rod: Molecular Basis for Cross-Linking of Actin Filaments. cell *98*, 10.

Dobbelaere, J., and Barral, Y. (2004). Spatial coordination of cytokinetic events by compartmentalization of the cell cortex. Science *305*, 393-396.
Dominguez, R. (2004). Actin-binding proteins--a unifying hypothesis. Trends Biochem Sci *29*, 572-578.

dos Remedios, C.G., Chhabra, D., Kekic, M., Dedova, I.V., Tsubakihara, M., Berry, D.A., and Nosworthy, N.J. (2003). Actin binding proteins: regulation of cytoskeletal microfilaments. Physiol Rev *83*, 433-473.

Douglas, M.E., Davies, T., Joseph, N., and Mishima, M. (2010). Aurora B and 14-3-3 coordinately regulate clustering of centralspindlin during cytokinesis. Curr Biol *20*, 927-933.

Estey, M.P., Di Ciano-Oliveira, C., Froese, C.D., Bejide, M.T., and Trimble, W.S. (2010). Distinct roles of septins in cytokinesis: SEPT9 mediates midbody abscission. J Cell Biol *191*, 741-749.

Fankhauser, C., Reymond, A., CerutU, L., Utzig, S., Hofmann, K., and Simanis, V. (1995). The Role of Cdc42p GTPase-activating Proteins in Assembly of the Septin Ring in Yeast. Cell *82*, 10.

Foth, B.J., Goedecke, M.C., and Soldati, D. (2006). New insights into myosin evolution and classification. Proc Natl Acad Sci U S A *103*, 3681-3686.

Fuller, B.G., Lampson, M.A., Foley, E.A., Rosasco-Nitcher, S., Le, K.V., Tobelmann, P., Brautigan, D.L., Stukenberg, P.T., and Kapoor, T.M. (2008). Midzone activation of aurora B in anaphase produces an intracellular phosphorylation gradient. Nature *453*, 1132-1136.

Gaillard, J., Neumann, E., Van Damme, D., Stoppin-Mellet, V., Ebel, C., Barbier, E., Geelen, D., and Vantard, M. (2008). Two microtubule-associated proteins of Arabidopsis MAP65s promote antiparallel microtubule bundling. Mol Biol Cell *19*, 4534-4544.

Geldner, N., Friml, J., Stierhof, Y.D., Jürgens, G., and Palme, K. (2001). Auxin transport inhibitors block PIN1 cycling and vesicle trafficking. Nature *413*, 425-428.

Gennerich, A., and Vale, R.D. (2009). Walking the walk: how kinesin and dynein coordinate their steps. Curr Opin Cell Biol *21*, 59-67.

Gladfelter, A.S., Bose, I., Zyla, T.R., Bardes, E.S., and Lew, D.J. (2002). Septin ring assembly involves cycles of GTP loading and hydrolysis by Cdc42p. J Cell Biol *156*, 315-326.

Glotzer, M. (2001). Animal cell cytokinesis. Annu Rev Cell Dev Biol *17*, 351-386.

Glotzer, M. (2009). The 3Ms of central spindle assembly: microtubules, motors and MAPs. Nat Rev Mol Cell Biol *10*, 9-20.

Glover, D.M., Ohkura, H., and Tavares, A. (1996). Polo kinase: the choreographer of the mitotic stage? J Cell Biol *135*, 1681-1684.

Goldschmidt-Clermont, P.J., Furman, M.I., Wachsstock, D., Safer, D., Nachmias, V.T., and Pollard, T.D. (1992). The control of actin nucleotide exchange by thymosin beta 4 and profilin. A potential regulatory mechanism for actin polymerization in cells. Mol Biol Cell *3*, 1015-1024.

Golji, J., Collins, R., and Mofrad, M.R. (2009). Molecular mechanics of the alpha-actinin rod domain: bending, torsional, and extensional behavior. PLoS Comput Biol *5*, e1000389.

Goode, B.L., Drubin, D.G., and Barnes, G. (2000). Functional cooperation between the microtubule and actin cytoskeletons. Curr Opin Cell Biol *12*, 63-71.

Granger, C.L., and Cyr, R.J. (2000). Microtubule reorganization in tobacco BY-2 cells stably expressing GFP-MBD. Planta *210*, 502-509.

Gregory, S.L., Ebrahimi, S., Milverton, J., Jones, W.M., Bejsovec, A., and Saint, R. (2008). Cell division requires a direct link between microtubule-bound RacGAP and Anillin in the contractile ring. Curr Biol *18*, 25-29.

Guha, M., Zhou, M., and Wang, Y.L. (2005). Cortical actin turnover during cytokinesis requires myosin II. Curr Biol *15*, 732-736.

Guizetti, J., and Gerlich, D.W. (2010). Cytokinetic abscission in animal cells. Semin Cell Dev Biol *21*, 909-916.

Guizetti, J., Schermelleh, L., Mäntler, J., Maar, S., Poser, I., Leonhardt, H., Müller-Reichert, T., and Gerlich, D.W. (2011). Cortical constriction during abscission involves helices of ESCRT-III-dependent filaments. Science *331*, 1616-1620.

Gunning, B.E.S., Hardham, A.R., and Hughes, J.E. (1978). Evidence for initiation of microtubules in discrete regions of the cell cortex in Azolla root-tip cells, and an hypothesis on the development of cortical arrays of microtubules. Planta *143*, 20.

Hardham, A.R., and Gunning, B.E. (1978). Structure of cortical microtubule arrays in plant cells. J Cell Biol *77*, 14-34.

Harkins, H.A., Page, N., Schenkman, L.R., Virgilio, C.D., Shaw, S., Bussey, H., and Pringle, J.R. (2001). Bud8p and Bud9p, Proteins That May Mark the Sites for Bipolar Budding in Yeast. Molecular Biology of Cell *12*, 22.

Hartman, M.A., and Spudich, J.A. (2012). The myosin superfamily at a glance. J Cell Sci *125*, 1627-1632.

Henne, W.M., Buchkovich, N.J., and Emr, S.D. (2011). The ESCRT pathway. Dev Cell *21*, 77-91.

Holy, T.E., and Leibler, S. (1994). Dynamic instability of microtubules as an efficient way to search in space. Proc Natl Acad Sci U S A *91*, 5682-5685.

Honda, K., Yamada, T., Endo, R., Ino, Y., Gotoh, M., Tsuda, H., Yamada, Y., Chiba, H., and Hirohashi, S. (1998). Actinin-4, a novel actin-bundling protein associated with cell motility and cancer invasion. J Cell Biol *140*, 1383-1393.

Hong, Z., Zhang, Z., Olson, J.M., and Verma, D.P. (2001). A novel UDP-glucose transferase is part of the callose synthase complex and interacts with phragmoplastin at the forming cell plate. Plant Cell *13*, 769-779.

Howard, J. (1997). Molecular motors: structural adaptations to cellular functions. Nature *389*, 561-567.

Hu, C.K., Coughlin, M., Field, C.M., and Mitchison, T.J. (2008). Cell polarization during monopolar cytokinesis. J Cell Biol *181*, 195-202.

Hurley, J.H., and Hanson, P.I. (2010). Membrane budding and scission by the ESCRT machinery: it's all in the neck. Nat Rev Mol Cell Biol *11*, 556-566.

Hutterer, A., Glotzer, M., and Mishima, M. (2009). Clustering of centralspindlin is essential for its accumulation to the central spindle and the midbody. Curr Biol *19*, 2043-2049.

Imamura, H., Tanaka, K., Hihara, T., Umikawa, M., Kamei, T., Takahashi, K., Sasaki, T., and Takai, Y. (1997). Bni1p and Bnr1p: downstream targets of the Rho family small G-proteins which interact with profilin and regulate actin cytoskeleton in Saccharomyces cerevisiae. EMBO J *16*, 2745-2755.

Ingouff, M., Fitz Gerald, J.N., Guérin, C., Robert, H., Sørensen, M.B., Van Damme, D., Geelen, D., Blanchoin, L., and Berger, F. (2005). Plant formin AtFH5 is an evolutionarily conserved actin nucleator involved in cytokinesis. Nat Cell Biol *7*, 374-380.

Janson, L.W., Sellers, J.R., and Taylor, a.D.L. (1992). Actin-Binding Proteins Regulate the Work Performed by Myosin I I Motors on Single Actin Filaments. Cell motility and Cytoskeleton *22*, 7.

Janson, M.E., Loughlin, R., Loïodice, I., Fu, C., Brunner, D., Nédélec, F.J., and Tran, P.T. (2007). Crosslinkers and motors organize dynamic microtubules to form stable bipolar arrays in fission yeast. Cell *128*, 357-368.

Jeyaprakash, A.A., Klein, U.R., Lindner, D., Ebert, J., Nigg, E.A., and Conti, E. (2007). Structure of a Survivin-Borealin-INCENP core complex reveals how chromosomal passengers travel together. Cell *131*, 271-285.

Jiang, W., Jimenez, G., Wells, N.J., Hope, T.J., Wahl, G.M., Hunter, T., and Fukunaga, R. (1998). PRC1: a human mitotic spindle-associated CDK substrate protein required for cytokinesis. Mol Cell *2*, 877-885.

Joo, E., Surka, M.C., and Trimble, W.S. (2007). Mammalian SEPT2 is required for scaffolding nonmuscle myosin II and its kinases. Dev Cell *13*, 677-690.

Jordan, M.A., and Wilson, L. (2004). Microtubules as a target for anticancer drugs. Nat Rev Cancer *4*, 253-265.

Jürgens, G. (2005). Cytokinesis in higher plants. Annu Rev Plant Biol *56*, 281-299.

Kamijo, K., Ohara, N., Abe, M., Uchimura, T., Hosoya, H., Lee, J.S., and Miki, T. (2006). Dissecting the role of Rho-mediated signaling in contractile ring formation. Mol Biol Cell *17*, 43-55.

Kosako, H., Yoshida, T., Matsumura, F., Ishizaki, T., Narumiya, S., and Inagaki, M. (2000). Rho-kinase/ROCK is involved in cytokinesis through the phosphorylation of myosin light chain and not ezrin/radixin/moesin proteins at the cleavage furrow. Oncogene *19*, 6.

Kunda, P., and Baum, B. (2009). The actin cytoskeleton in spindle assembly and positioning. Trends Cell Biol *19*, 174-179.

Laporte, D., Coffman, V.C., Lee, I.J., and Wu, J.Q. (2011). Assembly and architecture of precursor nodes during fission yeast cytokinesis. J Cell Biol *192*, 1005-1021.

Le Goff, X., Woollard, A., and Simanis, V. (1999). Analysis of the cps1 gene provides evidence for a septation checkpoint in Schizosaccharomyces pombe. Mol Gen Genet *262*, 163-172.

Lecuit, T., Lenne, P.F., and Munro, E. (2011). Force generation, transmission, and integration during cell and tissue morphogenesis. Annu Rev Cell Dev Biol *27*, 157-184.

Lewellyn, L., Carvalho, A., Desai, A., Maddox, A.S., and Oegema, K. (2011). The chromosomal passenger complex and centralspindlin independently contribute to contractile ring assembly. J Cell Biol *193*, 155-169.

Li, J., Wang, J., Jiao, H., Liao, J., and Xu, X. (2010). Cytokinesis and cancer: Polo loves ROCK'n' Rho(A). J Genet Genomics *37*, 159-172.

Liu, J., Tang, X., Wang, H., and Balasubramanian, M. (2000). Bgs2p, a 1,3-beta-glucan synthase subunit, is essential for maturation of ascospore wall in Schizosaccharomyces pombe. FEBS Lett *478*, 105-108.

Liu, J., Tang, X., Wang, H., Oliferenko, S., and Balasubramanian, M.K. (2002). The localization of the integral membrane protein Cps1p to the cell division site is dependent on the actomyosin ring and the septation-inducing network in Schizosaccharomyces pombe. Mol Biol Cell *13*, 989-1000.

Liu, J., Wang, H., McCollum, D., and Balasubramanian, M.K. (1999). Drc1p/Cps1p, a 1,3-beta-glucan synthase subunit, is essential for division septum assembly in Schizosaccharomyces pombe. Genetics *153*, 1193-1203.

Lord, M., Inose, F., Hiroko, T., Hata, T., Fujita, A., and Chant, J. (2002). Subcellular localization of Axl1, the cell type-specific regulator of polarity. Curr Biol *12*, 1347-1352.

Low, S.H., Li, X., Miura, M., Kudo, N., Quiñones, B., and Weimbs, T. (2003). Syntaxin 2 and endobrevin are required for the terminal step of cytokinesis in mammalian cells. Dev Cell *4*, 753-759.

Low, S.H., Mukhina, S., Srinivas, V., Ng, C.Z., and Murata-Hori, M. (2010). Domain analysis of alpha-actinin reveals new aspects of its association with F-actin during cytokinesis. Exp Cell Res *316*, 1925-1934.

Loïodice, I., Staub, J., Setty, T.G., Nguyen, N.P., Paoletti, A., and Tran, P.T. (2005). Ase1p organizes antiparallel microtubule arrays during interphase and mitosis in fission yeast. Mol Biol Cell *16*, 1756-1768.

Ma, X., Kovács, M., Conti, M.A., Wang, A., Zhang, Y., Sellers, J.R., and Adelstein, R.S. (2012). Nonmuscle myosin II exerts tension but does not translocate actin in vertebrate cytokinesis. Proc Natl Acad Sci U S A *109*, 4509-4514.

MA., C., S., K., and RS, A. (2008). Non-muscle myosin II. Myosins: A Superfamily of Molecular Motors. In: Proteins and Cell Regulation, ed. L.M. Coluccio, Berlin: Springer, 41.

Madaule, P., Eda, M., Watanabe, N., Fujisawa, K., Matsuoka, T., Bito, H., Ishizaki, T., and Narumiya, S. (1998). Role of citron kinase as a target of the small GTPase Rho in cytokinesis. Nature *394*, 491-494.

Maddox, A.S., Lewellyn, L., Desai, A., and Oegema, K. (2007). Anillin and the septins promote asymmetric ingression of the cytokinetic furrow. Dev Cell *12*, 827-835.

Matsumura, F. (2005). Regulation of myosin II during cytokinesis in higher eukaryotes. Trends Cell Biol *15*, 371-377.

Mckenna, N.M., and Wang, Y.L. (1989). Culturing cells on the microscope stage. Methods Cell Biol *29*, 195-205.

MINEYUKI, Y., MARC, J., and PALEVITZ, B.A. (1989). Development of the
preprophase band from random cytoplasmic microtubules in guard

mother cells of Allium. Planta *174*, 9.

Mishima, M., Kaitna, S., and Glotzer, M. (2002). Central spindle assembly and cytokinesis require a kinesin-like protein/RhoGAP complex with microtubule bundling activity. Dev Cell *2*, 41-54.

Mishra, M., and Oliferenko, S. (2008). Cytokinesis: catch and drag. Curr Biol *18*, R247-250.

Mitchison, T., and Kirschner, M. (1984). Dynamic instability of microtubule growth. Nature *312*, 237-242.

Miyauchi, K., Zhu, X., Foong, C., Hosoya, H., and Murata-Hori, M. (2007). Aurora B kinase activity is required to prevent polar cortical ingression during cytokinesis. Cell Cycle *6*, 2549-2553.

Molchan, T.M., Valster, A.H., and Hepler, P.K. (2002). Actomyosin promotes cell plate alignment and late lateral expansion in Tradescantia stamen hair cells. Planta *214*, 683-693.

Mollinari, C., Kleman, J.P., Saoudi, Y., Jablonski, S.A., Perard, J., Yen, T.J., and Margolis, R.L. (2005). Ablation of PRC1 by small interfering RNA demonstrates that cytokinetic abscission requires a central spindle bundle in mammalian cells, whereas completion of furrowing does not. Mol Biol Cell *16*, 1043-1055.

Morita, E. (2012). Differential requirements of mammalian ESCRTs in multivesicular body formation, virus budding and cell division. FEBS J *279*, 1399-1406.

Morrison, E.E., Wardleworth, B.N., Askham, J.M., Markham, A.F., and Meredith, D.M. (1998). EB1, a protein which interacts with the APC tumour suppressor, is associated with the microtubule cytoskeleton throughout the cell cycle. Oncogene *17*, 3471-3477.

Motegi, F., Mishra, M., Balasubramanian, M.K., and Mabuchi, I. (2004). Myosin-II reorganization during mitosis is controlled temporally by its dephosphorylation and spatially by Mid1 in fission yeast. J Cell Biol *165*, 685-695.

Mukhina, S., Wang, Y.L., and Murata-Hori, M. (2007). Alpha-actinin is required for tightly regulated remodeling of the actin cortical network during cytokinesis. Dev Cell *13*, 554-565.

Murata, T.W., M. (1991). Re-formation of the preprophase band after cold-induced depolymerization of microtubules in *Adiantum* protonemata. Plant Cell Physiol *32*, 7.

Murata-Hori, M., Tatsuka, M., and Wang, Y.L. (2002). Probing the dynamics and functions of aurora B kinase in living cells during mitosis and cytokinesis. Mol Biol Cell *13*, 1099-1108.

Murata-Hori, M., and Wang, Y.L. (2002). Both midzone and astral microtubules are involved in the delivery of cytokinesis signals: insights from the mobility of aurora B. J Cell Biol *159*, 45-53.

Murthy, K., and Wadsworth, P. (2005). Myosin-II-dependent localization and dynamics of F-actin during cytokinesis. Curr Biol *15*, 724-731.

Naumanen, P., Lappalainen, P., and Hotulainen, P. (2008). Mechanisms of actin stress fibre assembly. J Microsc *231*, 446-454.

Neto, H., and Gould, G.W. (2011). The regulation of abscission by multi-protein complexes. J Cell Sci *124*, 3199-3207.

Nishida, E., Maekawa, S., and Sakai, H. (1984). Cofilin, a protein in porcine brain that binds to actin filaments and inhibits their interactions with myosin and tropomyosin. Biochemistry *23*, 5307-5313.

Nishimura, Y., and Yonemura, S. (2006). Centralspindlin regulates ECT2 and RhoA accumulation at the equatorial cortex during cytokinesis. J Cell Sci *119*, 104-114.

Nislow, C., Sellitto, C., Kuriyama, R., and McIntosh, J.R. (1990). A monoclonal antibody to a mitotic microtubule-associated protein blocks mitotic progression. J Cell Biol *111*, 511-522.

O'Connell, C.B., Warner, A.K., and Wang, Y. (2001). Distinct roles of the equatorial and polar cortices in the cleavage of adherent cells. Curr Biol *11*, 702-707.

Otey, C.A., and Carpen, O. (2004). Alpha-actinin revisited: a fresh look at an old player. Cell Motil Cytoskeleton *58*, 104-111.

Paavilainen, V.O., Bertling, E., Falck, S., and Lappalainen, P. (2004). Regulation of cytoskeletal dynamics by actin-monomer-binding proteins. Trends Cell Biol *14*, 386-394.

Padmanabhan, A., Bakka, K., Sevugan, M., Naqvi, N.I., D'souza, V., Tang, X., Mishra, M., and Balasubramanian, M.K. (2011). IQGAP-related Rng2p organizes cortical nodes and ensures position of cell division in fission yeast. Curr Biol *21*, 467-472.

Paoletti, A., and Chang, F. (2000). Analysis of mid1p, a protein required for placement of the cell division site, reveals a link between the nucleus and the cell surface in fission yeast. Mol Biol Cell *11*, 2757-2773.

Parent, C.A. (2004). Making all the right moves: chemotaxis in neutrophils and Dictyostelium. Curr Opin Cell Biol *16*, 4-13.

Park, H.O., Chant, J., and Herskowitz, I. (1993). BUD2 encodes a GTPase-activating protein for Bud1/Rsr1 necessary for proper bud-site selection in yeast. Nature *365*, 269-274.

Park, H.O., Sanson, A., and Herskowitz, I. (1999). Localization of Bud2p, a GTPase-activating protein necessary for programming cell polarity in yeast to the presumptive bud site. Genes Dev *13*, 1912-1917.

Pavicic-Kaltenbrunner, V., Mishima, M., and Glotzer, M. (2007). Cooperative assembly of CYK-4/MgcRacGAP and ZEN-4/MKLP1 to form the centralspindlin complex. Mol Biol Cell *18*, 4992-5003.

Pelham, R.J., and Chang, F. (2002). Actin dynamics in the contractile ring during cytokinesis in fission yeast. Nature *419*, 82-86.

Peng, J., Wallar, B.J., Flanders, A., Swiatek, P.J., and Alberts, A.S. (2003). Disruption of the Diaphanous-related formin Drf1 gene encoding mDia1 reveals a role for Drf3 as an effector for Cdc42. Curr Biol *13*, 534-545.

Piekny, A., Werner, M., and Glotzer, M. (2005). Cytokinesis: welcome to the Rho zone. Trends Cell Biol *15*, 651-658.

Piekny, A.J., and Glotzer, M. (2008). Anillin is a scaffold protein that links RhoA, actin, and myosin during cytokinesis. Curr Biol *18*, 30-36.

Powers, J., Bossinger, O., Rose, D., Strome, S., and Saxton, W. (1998). A nematode kinesin required for cleavage furrow advancement. Curr Biol *8*, 1133-1136.

Prekeris, R., and Gould, G.W. (2008). Breaking up is hard to do - membrane traffic in cytokinesis. J Cell Sci *121*, 1569-1576.

R., Y., and K., N. (2001). A comprehesive expression analysis of all members of a gene family encoding cell-wall enzymes allowed us to predict cis-

regulatory regions involved in cell-wall construction in specific organs of Arabidopis. Plant Cell Physiol. *42*, 9.

Raich, W.B., Moran, A.N., Rothman, J.H., and Hardin, J. (1998). Cytokinesis and midzone microtubule organization in Caenorhabditis elegans require the kinesin-like protein ZEN-4. Mol Biol Cell *9*, 2037-2049.

RAPPAPORT, R. (1961). Experiments concerning the cleavage stimulus in sand dollar eggs. J Exp Zool *148*, 81-89.

Reichl, E.M., Ren, Y., Morphew, M.K., Delannoy, M., Effler, J.C., Girard, K.D., Divi, S., Iglesias, P.A., Kuo, S.C., and Robinson, D.N. (2008). Interactions between myosin and actin crosslinkers control cytokinesis contractility dynamics and mechanics. Curr Biol *18*, 471-480.

Reichl, E.M., and Robinson, D.N. (2007). Putting the brakes on cytokinesis with alpha-actinin. Dev Cell *13*, 460-462.

Reid, E., Connell, J., Edwards, T.L., Duley, S., Brown, S.E., and Sanderson, C.M. (2005). The hereditary spastic paraplegia protein spastin interacts with the ESCRT-III complex-associated endosomal protein CHMP1B. Hum Mol Genet *14*, 19-38.

Revenu, C., Athman, R., Robine, S., and Louvard, D. (2004). The co-workers of actin filaments: from cell structures to signals. Nat Rev Mol Cell Biol *5*, 635-646.

Ross, J.L., Shuman, H., Holzbaur, E.L., and Goldman, Y.E. (2008). Kinesin and dynein-dynactin at intersecting microtubules: motor density affects dynein function. Biophys J *94*, 3115-3125.

Ruchaud, S., Carmena, M., and Earnshaw, W.C. (2007). The chromosomal passenger complex: one for all and all for one. Cell *131*, 230-231.

Saito, S., Liu, X.F., Kamijo, K., Raziuddin, R., Tatsumoto, T., Okamoto, I., Chen, X., Lee, C.C., Lorenzi, M.V., Ohara, N., and Miki, T. (2004). Deregulation and mislocalization of the cytokinesis regulator ECT2 activate the Rho signaling pathways leading to malignant transformation. J Biol Chem *279*, 7169-7179.

Schiel, J.A., and Prekeris, R. (2010). Making the final cut - mechanisms mediating the abscission step of cytokinesis. ScientificWorldJournal *10*, 1424-1434.

Schroeder, T.E. (1972). The contractile ring. II. Determining its brief existence, volumetric changes, and vital role in cleaving Arbacia eggs. J Cell Biol *53*, 419-434.

Seguí-Simarro, J.M., Austin, J.R., White, E.A., and Staehelin, L.A. (2004). Electron tomographic analysis of somatic cell plate formation in meristematic cells of Arabidopsis preserved by high-pressure freezing. Plant Cell *16*, 836-856.

Sellitto, C., and Kuriyama, R. (1988). Distribution of a matrix component of the midbody during the cell cycle in Chinese hamster ovary cells. J Cell Biol *106*, 431-439.

Severson, A.F., Baillie, D.L., and Bowerman, B. (2002). A Formin Homology protein and a profilin are required for cytokinesis and Arp2/3-independent assembly of cortical microfilaments in C. elegans. Curr Biol *12*, 2066-2075.

Severson, A.F., Hamill, D.R., Carter, J.C., Schumacher, J., and Bowerman, B. (2000). The aurora-related kinase AIR-2 recruits ZEN-4/CeMKLP1 to the mitotic spindle at metaphase and is required for cytokinesis. Curr Biol *10*, 1162-1171.

Shannon, K.B., Canman, J.C., Ben Moree, C., Tirnauer, J.S., and Salmon, E.D. (2005). Taxol-stabilized microtubules can position the cytokinetic furrow in mammalian cells. Mol Biol Cell *16*, 4423-4436.

Shuster, C.B., and Burgess, D.R. (1999). Parameters that specify the timing of cytokinesis. J Cell Biol *146*, 981-992.

Sipiczki, M., Yamaguchi, M., Grallert, A., Takeo, K., Zilahi, E., Bozsik, A., and Miklos, I. (2000). Role of cell shape in determination of the division plane in Schizosaccharomyces pombe: random orientation of septa in spherical cells. J Bacteriol *182*, 1693-1701.

Skop, A.R., Liu, H., Yates, J., Meyer, B.J., and Heald, R. (2004). Dissection of the mammalian midbody proteome reveals conserved cytokinesis mechanisms. Science *305*, 61-66.

Sohrmann, M., Fankhauser, C., Brodbeck, C., and Simanis, V. (1996). The dmfl/midl gene is essential for correct positioning of the division septum in fission yeast. Genes and Development *10*, 13.

Staehelin, L.A., and Hepler, P.K. (1996). Cytokinesis in higher plants. Cell *84*, 821-824.

Steigemann, P., and Gerlich, D.W. (2009). Cytokinetic abscission: cellular dynamics at the midbody. Trends Cell Biol *19*, 606-616.

Straight, A.F., Cheung, A., Limouze, J., Chen, I., Westwood, N.J., Sellers, J.R., and Mitchison, T.J. (2003). Dissecting temporal and spatial control of cytokinesis with a myosin II Inhibitor. Science *299*, 1743-1747.

Tempel, M., Isenberg, G., and Sackmann, E. (1996). Temperature-induced sol-gel transition and microgel formation in alpha-actinin cross-linked actin networks: A rheological study. Physical Review E *54*, 9.

Tirnauer, J.S., Canman, J.C., Salmon, E.D., and Mitchison, T.J. (2002). EB1 targets to kinetochores with attached, polymerizing microtubules. Mol Biol Cell *13*, 4308-4316.

Tolic-Nørrelykke, I.M., Sacconi, L., Stringari, C., Raabe, I., and Pavone, F.S. (2005). Nuclear and division-plane positioning revealed by optical micromanipulation. Curr Biol *15*, 1212-1216.

Tolliday, N., VerPlank, L., and Li, R. (2002). Rho1 directs formin-mediated actin ring assembly during budding yeast cytokinesis. Curr Biol *12*, 1864-1870.

Tominaga, T., Sahai, E., Chardin, P., McCormick, F., Courtneidge, S.A., and Alberts, A.S. (2000). Diaphanous-related formins bridge Rho GTPase and Src tyrosine kinase signaling. Mol Cell *5*, 13-25.

Touré, A., Dorseuil, O., Morin, L., Timmons, P., Jégou, B., Reibel, L., and Gacon, G. (1998). MgcRacGAP, a new human GTPase-activating protein for Rac and Cdc42 similar to Drosophila rotundRacGAP gene product, is expressed in male germ cells. J Biol Chem *273*, 6019-6023.

Vale, R.D., Spudich, J.A., and Griffis, E.R. (2009). Dynamics of myosin, microtubules, and Kinesin-6 at the cortex during cytokinesis in Drosophila S2 cells. J Cell Biol *186*, 727-738.

Valster, A.H., Pierson, E.S., Valenta, R., Hepler, P.K., and Emons, A. (1997). Probing the Plant Actin Cytoskeleton during Cytokinesis and Interphase by Profilin Microinjection. Plant Cell *9*, 1815-1824.

Vavylonis, D., Wu, J.Q., Hao, S., O'Shaughnessy, B., and Pollard, T.D. (2008). Assembly mechanism of the contractile ring for cytokinesis by fission yeast. Science *319*, 97-100.

Wachsstock, D.H., Schwarz, W.H., and Pollard, T.D. (1993). Affinity of a-Actinin for Actin Determines the Structure and Mechanical Properties of Actin Filament Gels. Biophysical Journal *65*, 10.

Watanabe, S., Ando, Y., Yasuda, S., Hosoya, H., Watanabe, N., Ishizaki, T., and Narumiya, S. (2008). mDia2 induces the actin scaffold for the contractile ring and stabilizes its position during cytokinesis in NIH 3T3 cells. Mol Biol Cell *19*, 2328-2338.

Wheatley, S.P., Hinchcliffe, E.H., Glotzer, M., Hyman, A.A., Sluder, G., and Wang, Y. (1997). CDK1 inactivation regulates anaphase spindle dynamics and cytokinesis in vivo. J Cell Biol *138*, 385-393.

Winder, S.J., and Ayscough, K.R. (2005). Actin-binding proteins. J Cell Sci *118*, 651-654.

Wu, J.-Q., Ba¨hler, J.r., and Pringle, J.R. (2001). Roles of a Fimbrin and an a-Actinin-like Protein in Fission Yeast Cell Polarization and Cytokinesis. Molecular Biology of Cell *12*, 17.

Wu, J.Q., Kuhn, J.R., Kovar, D.R., and Pollard, T.D. (2003). Spatial and temporal pathway for assembly and constriction of the contractile ring in fission yeast cytokinesis. Dev Cell *5*, 723-734.

Wu, J.Q., Sirotkin, V., Kovar, D.R., Lord, M., Beltzner, C.C., Kuhn, J.R., and Pollard, T.D. (2006). Assembly of the cytokinetic contractile ring from a broad band of nodes in fission yeast. J Cell Biol *174*, 391-402.

Xu, J., Wirtz, D., and Pollard, T.D. (1998). Dynamic cross-linking by alpha-actinin determines the mechanical properties of actin filament networks. J Biol Chem *273*, 9570-9576.

Yamashiro, S., Totsukawa, G., Yamakita, Y., Sasaki, Y., Madaule, P., Ishizaki, T., Narumiya, S., and Matsumura, F. (2003). Citron kinase, a Rho-

dependent kinase, induces di-phosphorylation of regulatory light chain of myosin II. Mol Biol Cell *14*, 1745-1756.

Yang, D., Rismanchi, N., Renvoisé, B., Lippincott-Schwartz, J., Blackstone, C., and Hurley, J.H. (2008). Structural basis for midbody targeting of spastin by the ESCRT-III protein CHMP1B. Nat Struct Mol Biol *15*, 1278-1286.

Yokoyama, R., and Nishitani, K. (2001). A comprehensive expression analysis of all members of a gene family encoding cell-wall enzymes allowed us to predict cis-regulatory regions involved in cell-wall construction in specific organs of Arabidopsis. Plant Cell Physiol *42*, 1025-1033.

Yoshigaki, T. (1999). Simulation of density gradients of astral microtubules at cell surface in cytokinesis of sea urchin eggs. J Theor Biol *196*, 211-224.

Young, P., and Gautel, M. (2000). The interaction of titin and alpha-actinin is controlled by a phospholipid-regulated intramolecular pseudoligand mechanism. EMBO J *19*, 6331-6340.

Yumura, S., Ueda, M., Sako, Y., Kitanishi-Yumura, T., and Yanagida, T. (2008). Multiple mechanisms for accumulation of myosin II filaments at the equator during cytokinesis. Traffic *9*, 2089-2099.

Yüce, O., Piekny, A., and Glotzer, M. (2005). An ECT2-centralspindlin complex regulates the localization and function of RhoA. J Cell Biol *170*, 571-582.

Zhang, D., Wadsworth, P., and Helper, P.K. (1993). Dynamics of microfilaments are similar, but distinct from, microtubules during cytokinesis in living, diving plant cells. Cell Motil. Cytoskeleton *24*, 5.

Zhang, W., and Gunst, S.J. (2006). Dynamic association between alpha-actinin and beta-integrin regulates contraction of canine tracheal smooth muscle. J Physiol *572*, 659-676.

Zhao, W.M., and Fang, G. (2005). MgcRacGAP controls the assembly of the contractile ring and the initiation of cytokinesis. Proc Natl Acad Sci U S A *102*, 13158-13163.

Zhou, M., and Wang, Y.L. (2008). Distinct pathways for the early recruitment of myosin II and actin to the cytokinetic furrow. Mol Biol Cell *19*, 318-326.

Zhu, C., and Jiang, W. (2005). Cell cycle-dependent translocation of PRC1 on the spindle by Kif4 is essential for midzone formation and cytokinesis. Proc Natl Acad Sci U S A *102*, 343-348.

Zumdieck, A., Kruse, K., Bringmann, H., Hyman, A.A., and Jülicher, F. (2007). Stress generation and filament turnover during actin ring constriction. PLoS One *2*, e696.

Figure 1

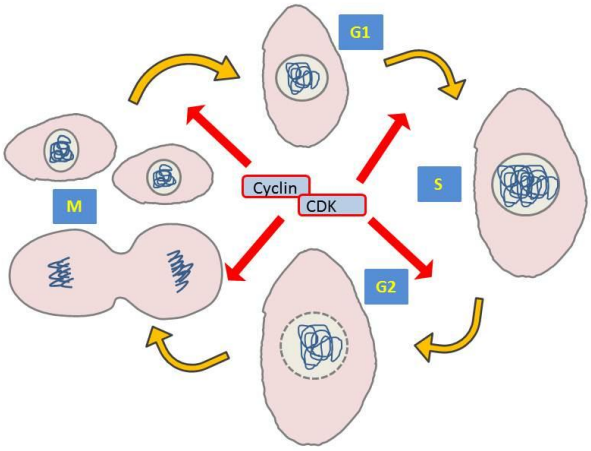

Figure 2

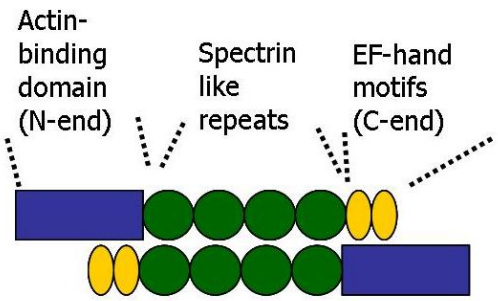

α-actinin homodimer

Figure 3

a)

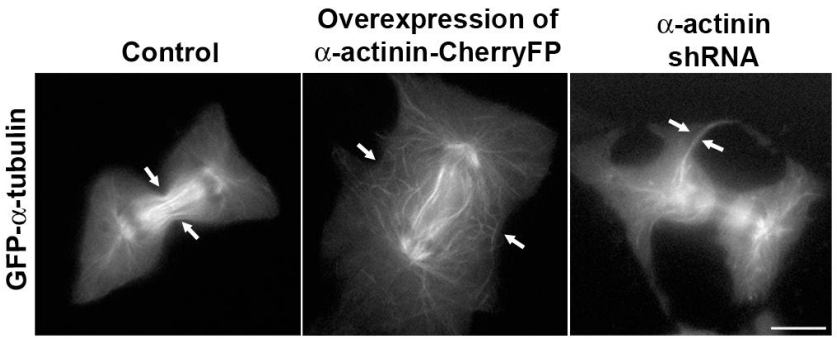
Control
Overexpression of α-actinin-CherryFP
α-actinin shRNA
GFP-α-tubulin

b)

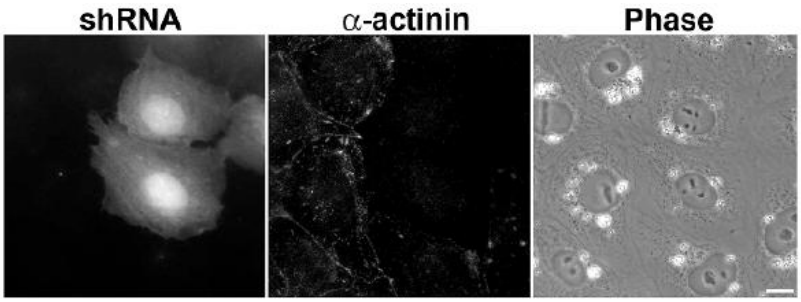
shRNA
α-actinin
Phase

c)

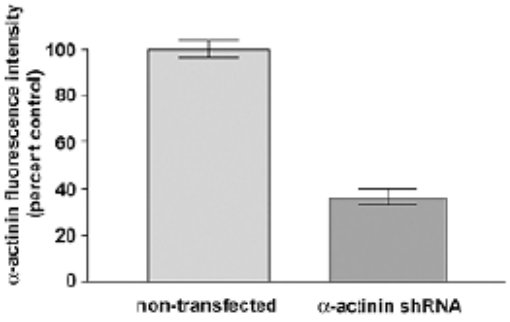
α-actinin fluorescence intensity (percent control)
100
80
60
40
20
0
non-transfected
α-actinin shRNA

Figure 4

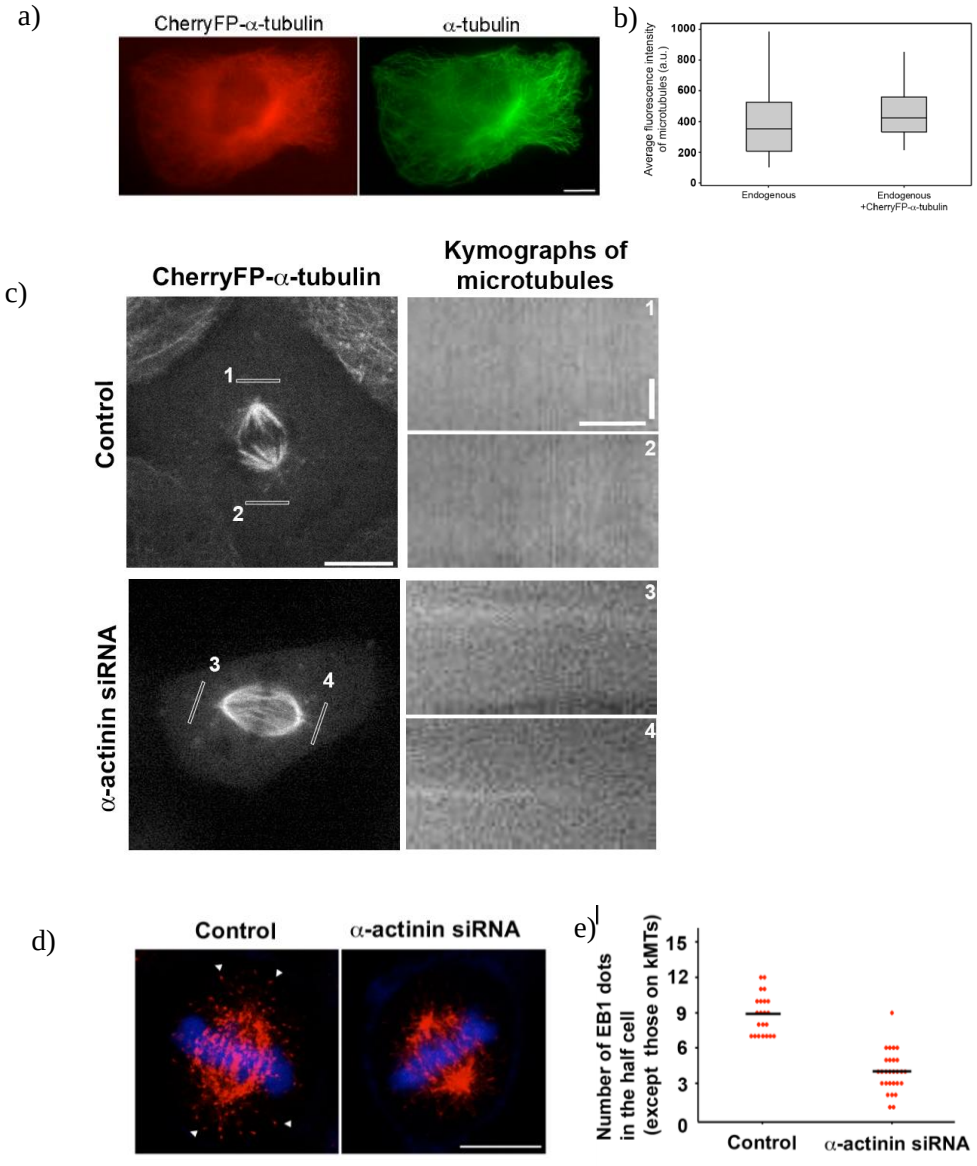
a)
CherryFP-α-tubulin
α-tubulin
b)
Average fluorescence intensity of microtubules (a.u.)
1000
800
600
400
200
0
Endogenous
Endogenous +CherryFP-α-tubulin
c)
CherryFP-α-tubulin
Kymographs of microtubules
Control
α-actinin siRNA
1
2
3
4
d)
Control
α-actinin siRNA
e)
Number of EB1 dots in the half cell (except those on kMTs)
15
12
9
6
3
0
Control
α-actinin siRNA

Figure 5

a)

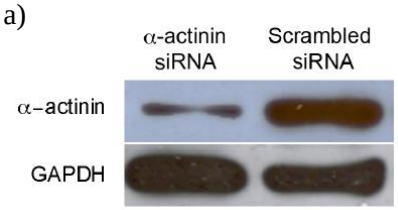

b)

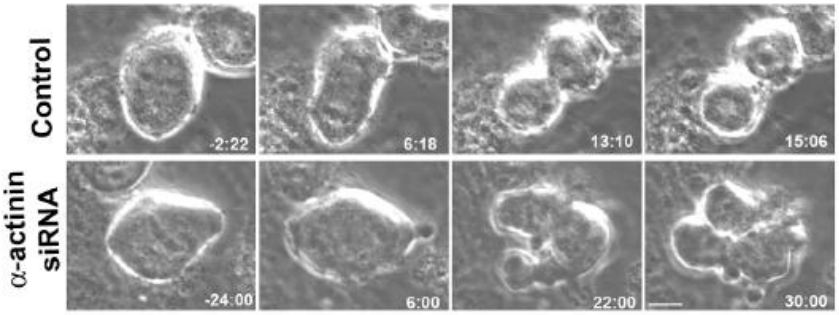

c)

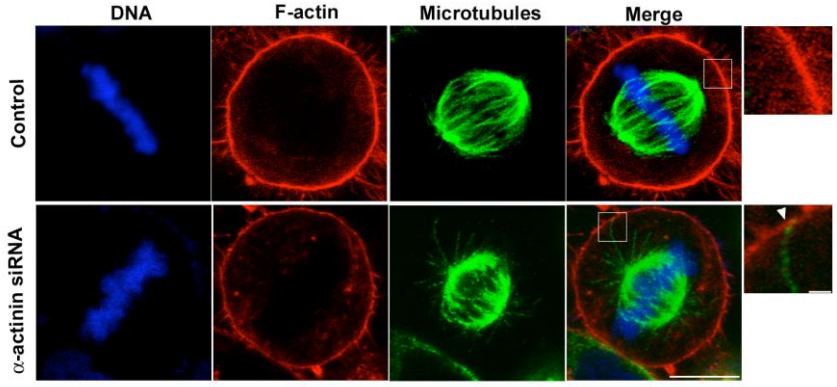

d)

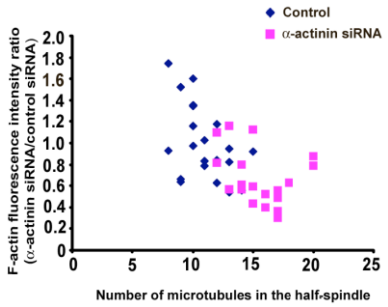

Figure 6

a)

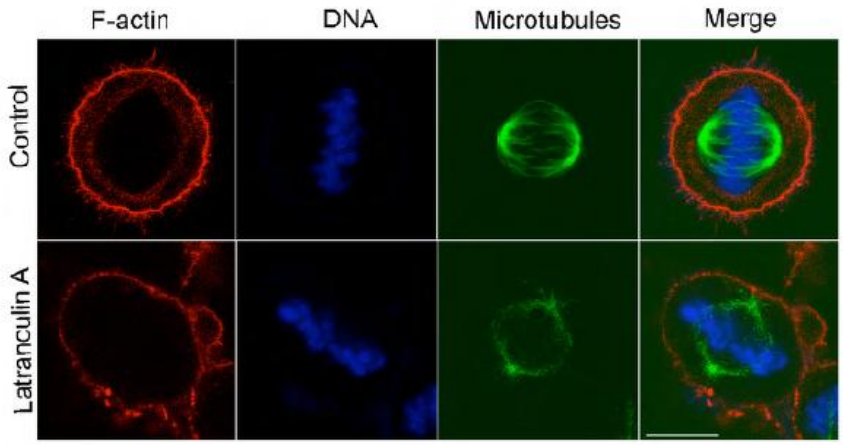
F-actin
DNA
Microtubules
Merge
Control
Latranculin A

b)

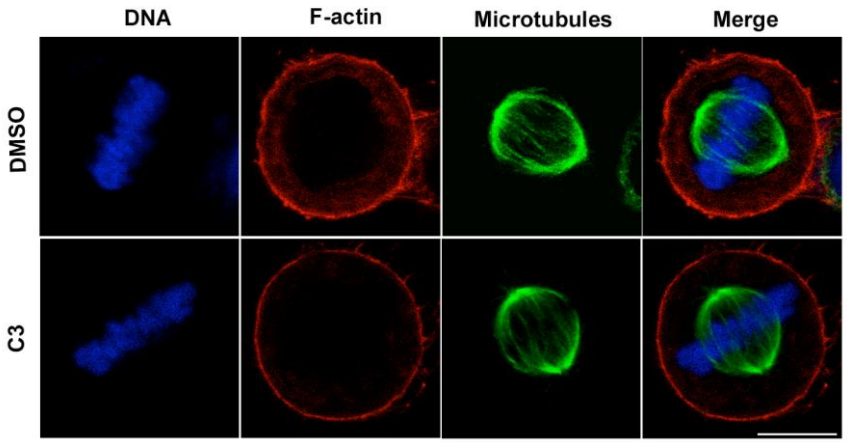
DNA
F-actin
Microtubules
Merge
DMSO
C3

c)

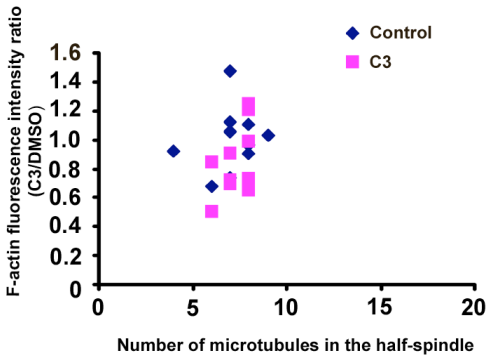
Control
C3
F-actin fluorescence intensity ratio (C3/DMSO)
1.6
1.4
1.2
1.0
0.8
0.6
0.4
0.2
0
0
5
10
15
20
Number of microtubules in the half-spindle

Figure 7

a)

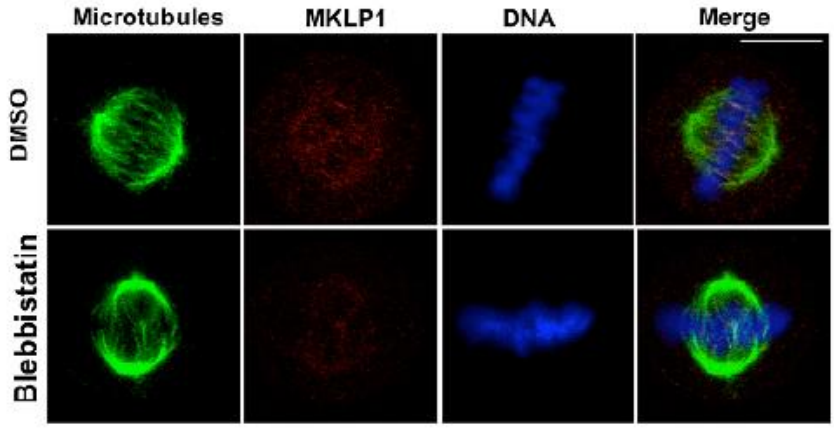
Microtubules
MKLP1
DNA
Merge
DMSO
Blebbistatin

b)

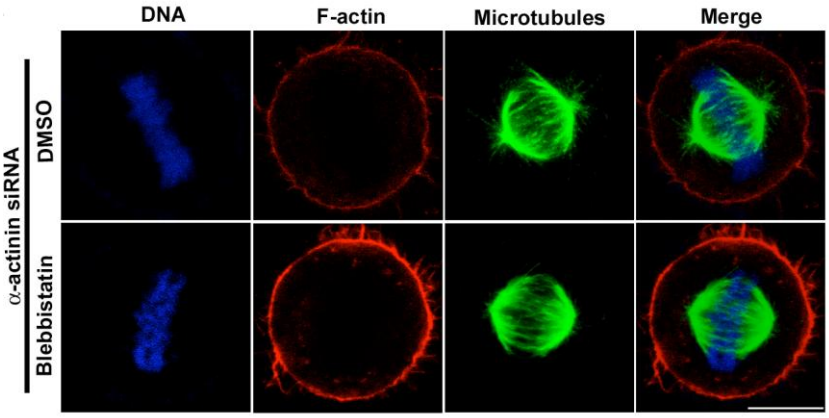
DNA
F-actin
Microtubules
Merge
α-actinin siRNA
DMSO
Blebbistatin

c)

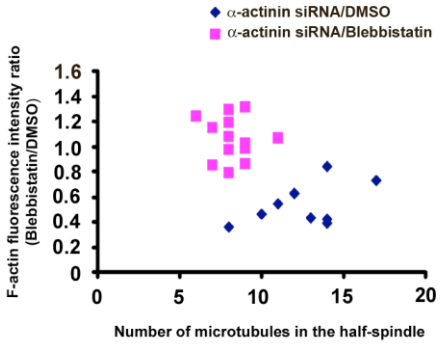
α-actinin siRNA/DMSO
α-actinin siRNA/Blebbistatin
F-actin fluorescence intensity ratio (Blebbistatin/DMSO)
1.6
1.4
1.2
1.0
0.8
0.6
0.4
0.2
0
0
5
10
15
20
Number of microtubules in the half-spindle

Figure 8

a)

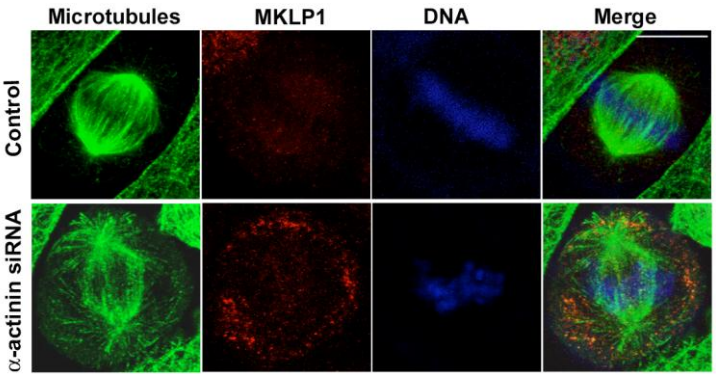

b)

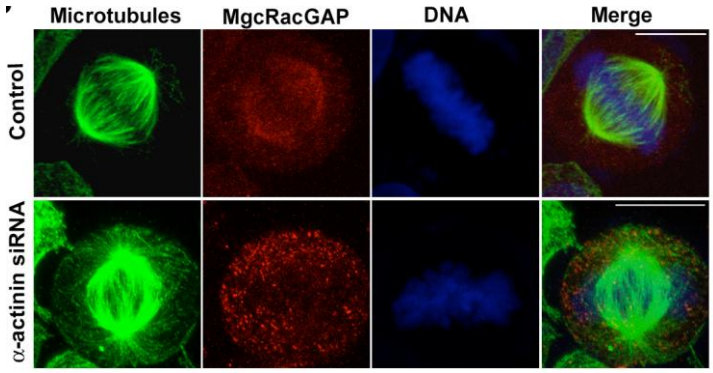

c)

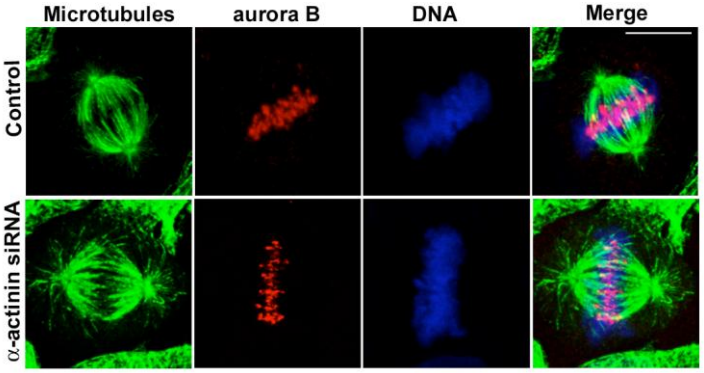

d)

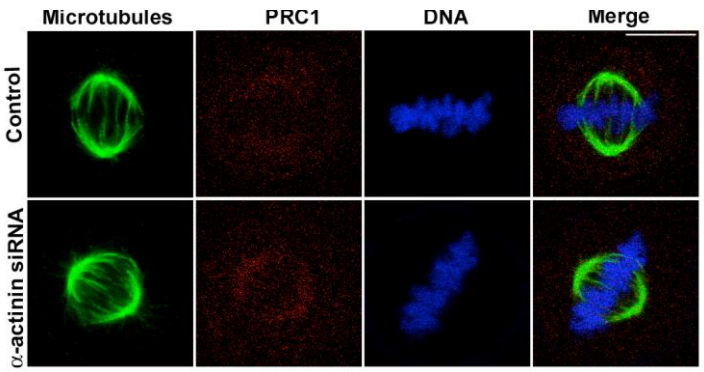

Figure 9

a)

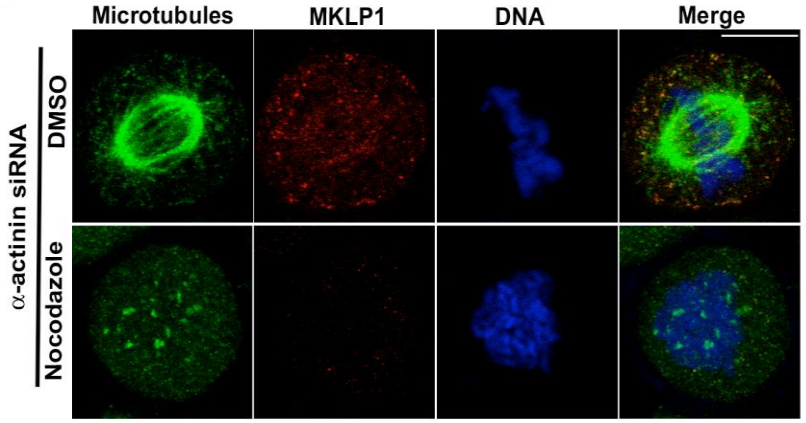
Microtubules
MKLP1
DNA
Merge
α-actinin siRNA
DMSO
Nocodazole

b)

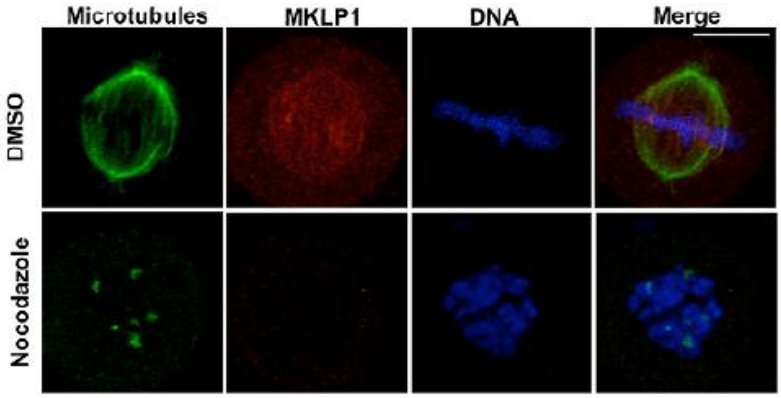
Microtubules
MKLP1
DNA
Merge
DMSO
Nocodazole

Figure 10

a)

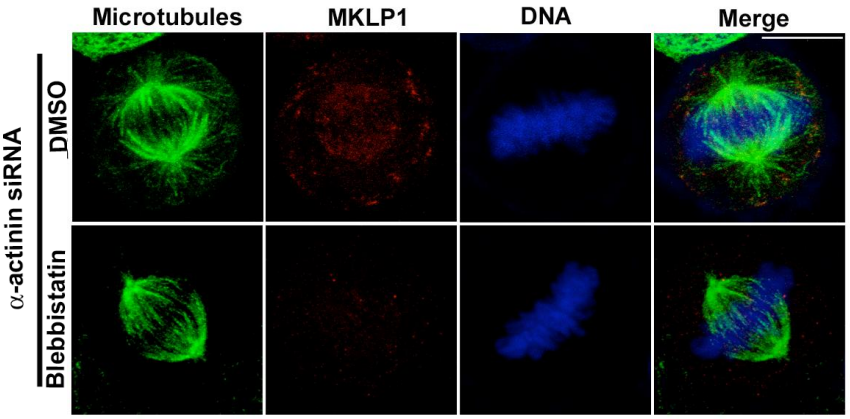
Microtubules
MKLP1
DNA
Merge
α-actinin siRNA
DMSO
Blebbistatin

b)

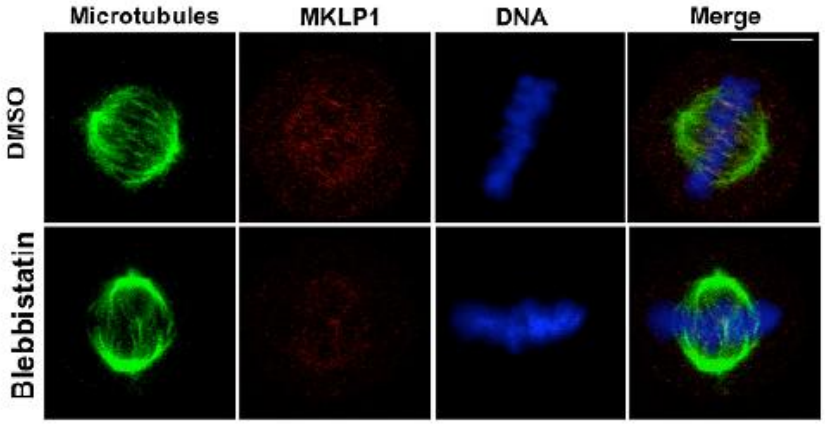
Microtubules
MKLP1
DNA
Merge
DMSO
Blebbistatin

Figure 11

a)

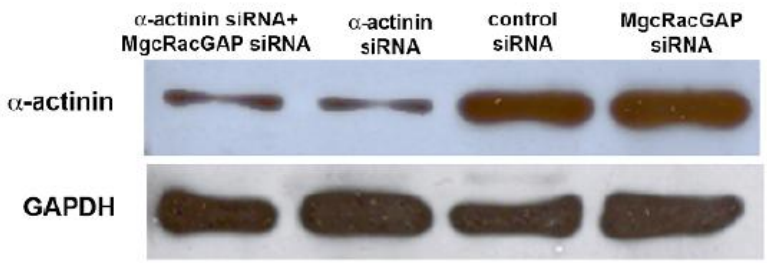

b)

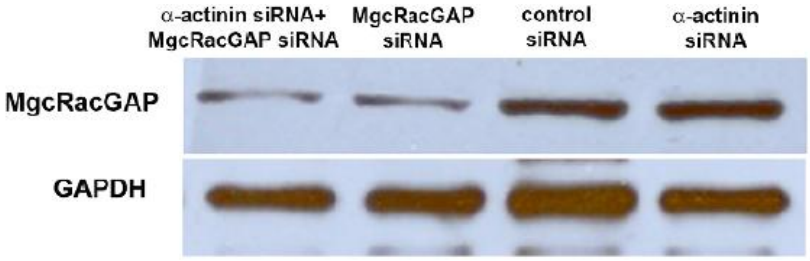

c)

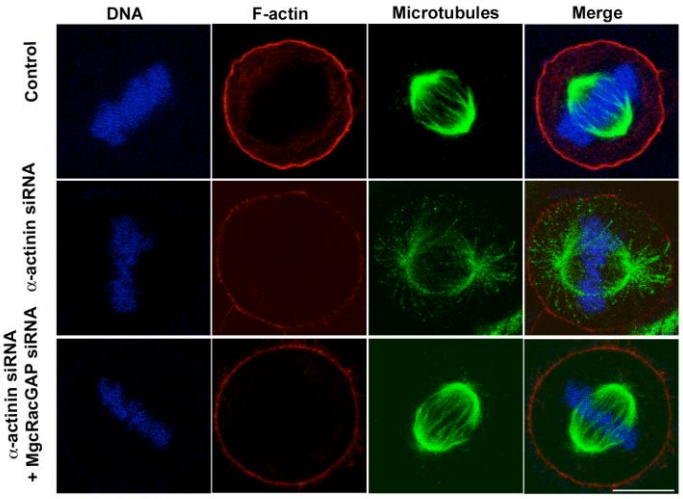

d)

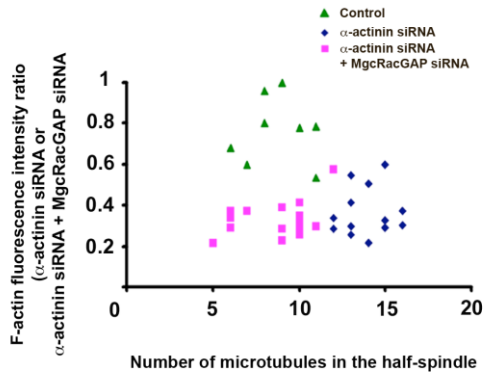

Figure 12

a)

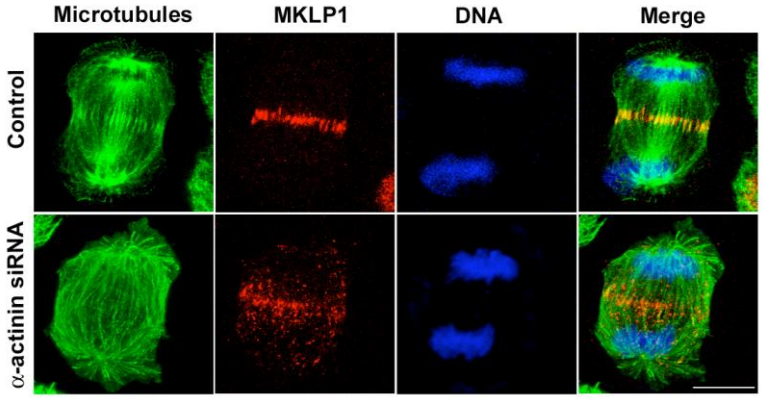
Microtubules
MKLP1
DNA
Merge
Control
α-actinin siRNA

b)

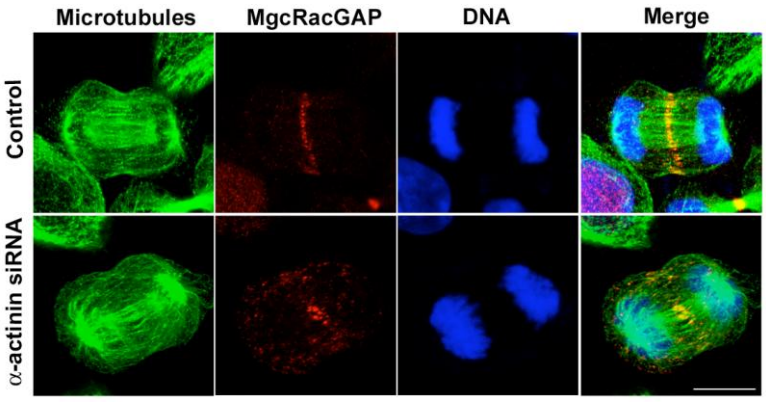
Microtubules
MgcRacGAP
DNA
Merge
Control
α-actinin siRNA

Figure 13

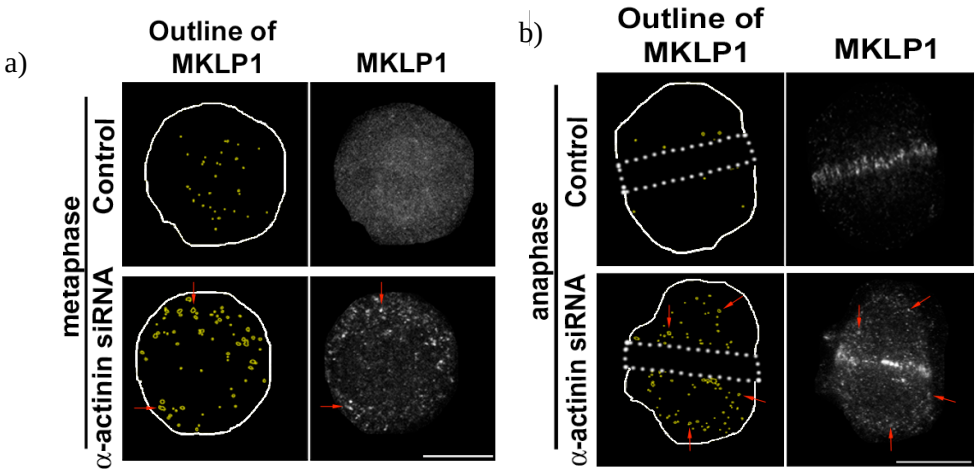
a)
Outline of MKLP1
MKLP1
metaphase
Control
α-actinin siRNA
b)
Outline of MKLP1
MKLP1
anaphase
Control
α-actinin siRNA

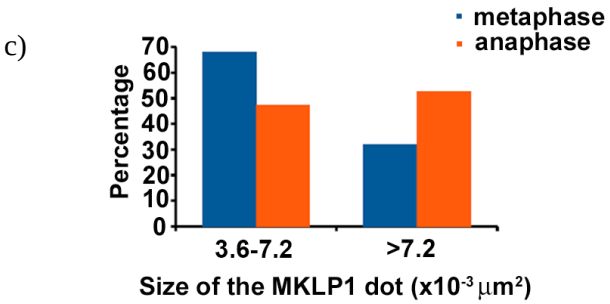
c)
metaphase
anaphase
Percentage
70
60
50
40
30
20
10
0
3.6-7.2
>7.2
Size of the MKLP1 dot (x10-3 μm2)

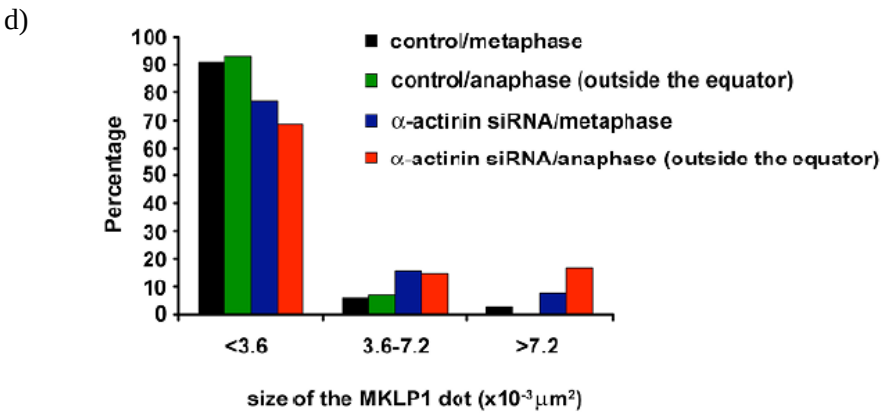
d)
control/metaphase
control/anaphase (outside the equator)
α-actinin siRNA/metaphase
α-actinin siRNA/anaphase (outside the equator)
Percentage
100
90
80
70
60
50
40
30
20
10
0
<3.6
3.6-7.2
>7.2
size of the MKLP1 dot (x10-3 μm2)

Figure 14

a)

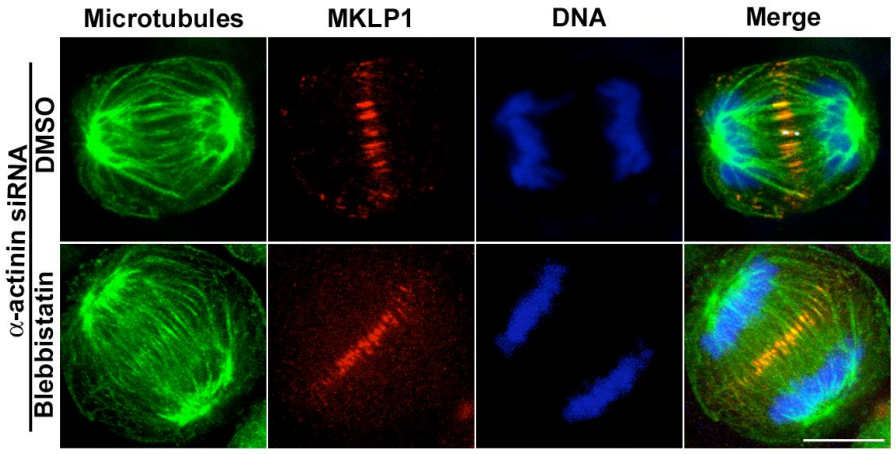
Microtubules
MKLP1
DNA
Merge
α-actinin siRNA
DMSO
Blebbistatin

b)

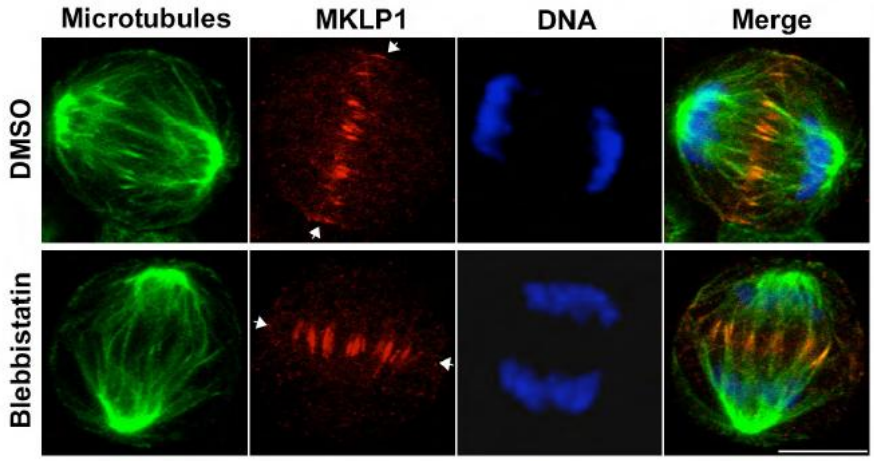
Microtubules
MKLP1
DNA
Merge
DMSO
Blebbistatin

Figure 15

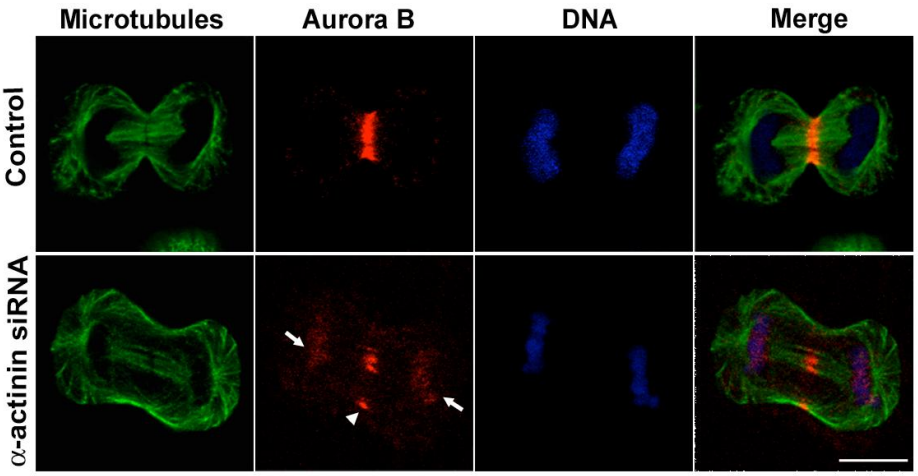

Figure 16

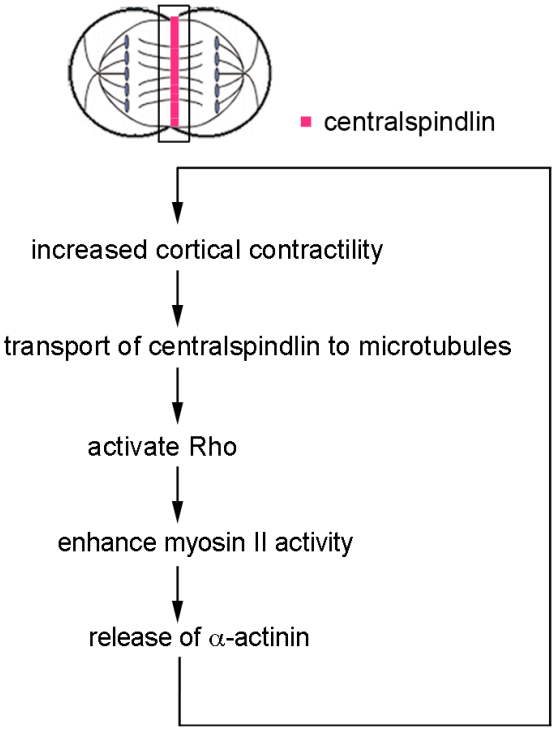
centralspindlin
increased cortical contractility
transport of centralspindlin to microtubules
activate Rho
enhance myosin II activity
release of α-actinin